OPTIMAL CHARGING INFRASTRUCTURE DESIGN FOR BATTERY ELECTRIC BUSES

FINAL PROJECT REPORT

by

Xuegang (Jeff) Ban, Dan McCabe
University of Washington

Sponsored by PacTrans and King County Metro Transit

for

Pacific Northwest Transportation Consortium (PacTrans)
USDOT University Transportation Center for Federal Region 10
University of Washington
More Hall 112, Box 352700
Seattle, WA 98195-2700

In cooperation with U.S. Department of Transportation,
Office of the Assistant Secretary for Research and Technology (OST-R)

DISCLAIMER

The contents of this report reflect the views of the authors, who are responsible for the facts and the accuracy of the information presented herein. This document is disseminated under the sponsorship of the U.S. Department of Transportation's University Transportation Centers Program, in the interest of information exchange. The Pacific Northwest Transportation Consortium, the U.S. Government and matching sponsor assume no liability for the contents or use thereof.

TECHNICAL REPORT DOCUMENTATION PAGE

1. Report No.	2. Government Accession No.	3. Recipient's Catalog No.
	01764501	

4. Title and Subtitle	5. Report Date:
Optimal Charging Infrastructure Design for Battery Electric Buses	09/01/2022
	6. Performing Organization Code

7. Author(s) and Affiliations	8. Performing Organization Report No.
Xuegang (Jeff) Ban, 0000-0001-8485-4799; Dan McCabe, 0000-0001-9971-9207; University of Washington	2020-S-UW-2

9. Performing Organization Name and Address	10. Work Unit No. (TRAIS)
PacTrans Pacific Northwest Transportation Consortium University Transportation Center for Federal Region 10 University of Washington More Hall 112 Seattle, WA 98195-2700	11. Contract or Grant No. 69A3551747110

12. Sponsoring Organization Name and Address	13. Type of Report and Period Covered
United States Department of Transportation Research and Innovative Technology Administration 1200 New Jersey Avenue, SE Washington, DC 20590	14. Sponsoring Agency Code

15. Supplementary Notes

Report uploaded to: www.pactrans.org

16. Abstract

Public transit agencies across the United States are rapidly converting their bus fleets from diesel or hybrid powertrains to battery-electric propulsion systems. To realize the benefits of this transition while retaining acceptable quality of service and limiting capital costs, agencies must intelligently decide where to locate recharging infrastructure. To address this challenge, this research developed two mixed-integer linear programming models that optimize the tradeoff between upfront charging infrastructure costs and operational performance in the form of trip delays and recovery times. A discrete-event simulation model was also developed to accurately quantify queue delays at heavily used chargers and to better evaluate system performance under real-world variations in key parameters such as bus energy consumption per mile. The models were applied to a case study of South King County, Washington, where an electric bus deployment is planned in the near future. The results showed that the models are effective at identifying sensible locations and ensuring that buses can charge without incurring additional delays. Limitations of the current research are also summarized, with future improvements discussed.

17. Key Words	18. Distribution Statement
Battery electric bus; charging location optimization; layover charging; mixed-integer linear program; simulation	

19. Security Classification (of this report)	20. Security Classification (of this page)	21. No. of Pages	22. Price
Unclassified.	Unclassified.	35	N/A

Form DOT F 1700.7 (8-72) **Reproduction of completed page authorized.**

SI* (MODERN METRIC) CONVERSION FACTORS

APPROXIMATE CONVERSIONS TO SI UNITS

Symbol	When You Know	Multiply By	To Find	Symbol
		LENGTH		
in	inches	25.4	millimeters	mm
ft	feet	0.305	meters	m
yd	yards	0.914	meters	m
mi	miles	1.61	kilometers	km
		AREA		
in^2	square inches	645.2	square millimeters	mm^2
ft^2	square feet	0.093	square meters	m^2
yd^2	square yard	0.836	square meters	m^2
ac	acres	0.405	hectares	ha
mi^2	square miles	2.59	square kilometers	km^2
		VOLUME		
fl oz	fluid ounces	29.57	milliliters	mL
gal	gallons	3.785	liters	L
ft^3	cubic feet	0.028	cubic meters	m^3
yd^3	cubic yards	0.765	cubic meters	m^3
	NOTE: volumes greater than 1000 L shall be shown in m^3			
		MASS		
oz	ounces	28.35	grams	g
lb	pounds	0.454	kilograms	kg
T	short tons (2000 lb)	0.907	megagrams (or "metric ton")	Mg (or "t")
		TEMPERATURE (exact degrees)		
°F	Fahrenheit	5 (F-32)/9 or (F-32)/1.8	Celsius	°C
		ILLUMINATION		
fc	foot-candles	10.76	lux	lx
fl	foot-Lamberts	3.426	$candela/m^2$	cd/m^2
		FORCE and PRESSURE or STRESS		
lbf	poundforce	4.45	newtons	N
lbf/in^2	poundforce per square inch	6.89	kilopascals	kPa

APPROXIMATE CONVERSIONS FROM SI UNITS

Symbol	When You Know	Multiply By	To Find	Symbol
		LENGTH		
mm	millimeters	0.039	inches	in
m	meters	3.28	feet	ft
m	meters	1.09	yards	yd
km	kilometers	0.621	miles	mi
		AREA		
mm^2	square millimeters	0.0016	square inches	in^2
m^2	square meters	10.764	square feet	ft^2
m^2	square meters	1.195	square yards	yd^2
ha	hectares	2.47	acres	ac
km^2	square kilometers	0.386	square miles	mi^2
		VOLUME		
mL	milliliters	0.034	fluid ounces	fl oz
L	liters	0.264	gallons	gal
m^3	cubic meters	35.314	cubic feet	ft^3
m^3	cubic meters	1.307	cubic yards	yd^3
		MASS		
g	grams	0.035	ounces	oz
kg	kilograms	2.202	pounds	lb
Mg (or "t")	megagrams (or "metric ton")	1.103	short tons (2000 lb)	T
		TEMPERATURE (exact degrees)		
°C	Celsius	1.8C+32	Fahrenheit	°F
		ILLUMINATION		
lx	lux	0.0929	foot-candles	fc
cd/m^2	$candela/m^2$	0.2919	foot-Lamberts	fl
		FORCE and PRESSURE or STRESS		
N	newtons	0.225	poundforce	lbf
kPa	kilopascals	0.145	poundforce per square inch	lbf/in^2

*SI is the symbol for the International System of Units. Appropriate rounding should be made to comply with Section 4 of ASTM E380.
(Revised March 2003)

TABLE OF CONTENTS

LIST OF FIGURES

LIST OF TABLES

LIST OF ABBREVIATIONS

AFV:	Alternative fuel vehicles
API:	Application programming interface
BEB:	Battery-electric buses
EV:	Electric vehicle
EVRP:	Electric vehicle routing problem
GTFS:	General Transit Feed Specification
LQ:	Linear queue
MILP:	Mixed-integer linear programming
NREL:	National Renewable Energy Laboratory
O-D:	Origin-destination
PacTrans:	Pacific Northwest Transportation Consortium
WSDOT:	Washington State Department of Transportation

ACKNOWLEDGMENTS

King County Metro Transit (Metro) provided matching funds for this project, which is greatly appreciated. Metro staff and managers also provided data, and valuable input regarding the direction of the research and the proposed modeling methods and results. The project team thanks them for their efforts, which ensured the successful completion of the project.

EXECUTIVE SUMMARY

Public transit agencies across the United States are rapidly converting their bus fleets from diesel or hybrid powertrains to battery-electric propulsion systems. To realize the benefits of this transition while retaining acceptable quality of service and limiting capital costs, agencies must intelligently decide where to locate recharging infrastructure. While most agencies electrifying their fleets plan to install chargers at bases where buses are kept overnight, a question faced by many fleet operators is where to install layover chargers that provide additional energy while buses are in operation during the day. To address this challenge, this research developed two mixed-integer linear programming models that optimize the tradeoff between upfront charging infrastructure costs and operational performance in the form of trip delays and recovery times. A discrete-event simulation model was also developed to accurately quantify queue delays at heavily used chargers and better evaluate system performance under real-world variations in key parameters such as bus energy consumption per mile. The models were applied to a case study of South King County, Washington, where an electric bus deployment is planned in the near future. The results showed that the models are effective at identifying sensible locations and ensuring that buses can charge without incurring additional delays.

The research results also indicated that the current models are not very robust to the uncertainty in key model parameters, such as the energy consumption rate of battery-electric buses (BEBs) or the charging performance at the stations. An ideal model would recognize that some of the parameters in the proposed models in this project are not known exactly and would seek to provide good system performance over a wide range of real-world scenarios. Several ideas, ranging from detailed simulation modeling to rigorous stochastic optimization, regarding how the current models may be improved to incorporate uncertainty modeling are presented and discussed.

While there are clear future directions for improvement, the models presented in this report should still provide value to agencies looking to develop their charging infrastructure and add to the growing body of literature on decision making for BEB charging infrastructure and operations. As transit electrification continues to take hold across the United States, such models will be increasingly important and will help accelerate a transition to more environmentally friendly transit vehicles in the Pacific Northwest region and across the U.S.

.

CHAPTER 1. INTRODUCTION

Transit agencies across the United States, supported by federal funding, have established ambitious goals to eliminate emissions in their bus fleets (Federal Transit Administration, 2015). In the Seattle area, for example, King County Metro Transit (hereafter referred to as Metro) has committed to operating a fully zero-emissions bus fleet by 2040 (King County Metro, 2020). Metro and other agencies plan to meet their emissions goals in large part with battery-electric buses (BEBs). BEBs, like other electric vehicles (EVs), are powered by battery packs that supply power to an electric motor. Because they produce no tailpipe emissions, BEBs powered by renewable energy sources are a promising technology to both reduce greenhouse gas emissions and decrease air pollution in urban areas. They can also have much lower lifetime energy costs in comparison to buses propelled by internal combustion engines, especially in areas with low electricity costs, and lower maintenance costs because of their comparatively simpler powertrains with fewer moving parts (Johnson, et al., 2020).

Although the environmental benefits of BEBs are clear (Ercan & Tatari, 2015; Nordelöf, et al., 2019; Shi, et al., 2019; Zhou, et al., 2016), their viability for serving existing transit systems depends on the existence of adequate charging infrastructure. Typical costs for chargers are in the tens of thousands of dollars (Johnson, et al., 2020), so agencies must take care in identifying charger locations in order to limit the number of chargers they must purchase while also ensuring that infrastructure is sufficient to meet service needs and minimize operational costs. Hence, locating charging stations intelligently can promote efficient and reliable operations while limiting capital costs, easing the transition from higher-emitting vehicles to BEBs.

In the infrastructure planning process, agencies need to determine not only where chargers are located but also how and when buses will be charged. A common strategy is to charge buses overnight as much as possible (Transportation Research Board and National Academies of Sciences, Engineering, and Medicine, 2018). This is a sensible approach for multiple reasons. First, most or all of an agency's buses are likely to be out of service overnight, allowing plenty of time to recharge batteries, which can take several hours depending on battery size and charger power output. Second, electricity prices are usually at their lowest overnight because demand is low (Transportation Research Board and National Academies of Sciences, Engineering, and Medicine, 2021). Third, it is relatively straightforward to install and operate

charging infrastructure at bus bases—making upgrades to bus facilities and electric grid connections at these sites is likely to be technically, financially, and logistically preferable in comparison to other sites. Accordingly, many agencies, including Metro, plan to install large numbers of bus chargers at bases where buses are parked overnight (King County Metro Transit, 2020).

While overnight charging is straightforward and often more cost effective than other approaches, this strategy alone may not be enough to serve all of an agency's routes each day. Metro anticipates that the range of BEBs with current battery technology is sufficient to serve about 70 percent of its bus assignments without requiring charging during the day (King County Metro Transit, 2020). The remaining 30 percent of buses would either need to alter their assignments or rely on supplemental charging in between trips during the day, which is referred to as *layover charging*. Although Metro has formalized its immediate plans for installing chargers at the interim bus base that will house its initial BEB fleet, when and where to deploy layover charging is still an open question for the agency (King County Metro Transit, 2020).

Inspired by this challenge faced by Metro and other agencies, the aim of this research project was to develop a decision-making tool that transit agencies seeking to electrify their fleets can use to identify ideal locations for layover charging infrastructure. Specifically, this work developed two similar optimization models for minimum-cost locating of charging infrastructure that are applicable to nearly any bus network and utilize readily available data. Part of Metro's service area in South King County, Washington, was used as a case study to demonstrate the models' potential usefulness to transit agencies, as well as their sensitivity to some key parameters.

1.1. Literature Review

1.1.1. Overview of BEB Technologies and Considerations

BEBs offer an array of benefits to transit operators that employ them. They are quieter and smoother in operation than their diesel and hybrid counterparts, have fewer moving parts, and eliminate tailpipe emissions that degrade urban air quality (Transportation Research Board and National Academies of Sciences, Engineering, and Medicine, 2018). Depending on procurement costs, electricity rates, and the efficiency of their operations, they may also offer financial benefits over conventionally fueled buses (Johnson, et al., 2020). Transit agencies across the United States have recognized these benefits and have begun to adopt BEBs at an

ever-increasing scale. As of 2018, at least 70 American transit agencies were operating BEBs, though often with small fleets in trial programs (Transportation Research Board and National Academies of Sciences, Engineering, and Medicine, 2018).

It is important to recognize that BEB deployment encompasses a wide range of technologies and operational strategies, each of which may be appropriate in the right context. These differences generally arise in response to two of the major challenges posed by Evs of all types: limited driving range and slow recharging times (in comparison to conventionally fueled vehicles). To mitigate the impacts of these challenges, BEB operators often choose one of two schemes: equipping buses with relatively large batteries and charging them slowly overnight so that they can complete daily service assignments without the need to recharge, or utilizing buses with relatively low-capacity batteries and recharging them frequently throughout the day at high power (Transportation Research Board and National Academies of Sciences, Engineering, and Medicine, 2018). A hybrid strategy is also possible, in which buses are charged slowly overnight while out of service and partially recharged during the service day during layover time (idle time between trips).

Regardless of the strategy employed for charging, BEB operators must also select an appropriate technology for charging. There are three main categories of charging systems for BEBs: plug-in, overhead conductive, and wireless (or *inductive*) (Transportation Research Board and National Academies of Sciences, Engineering, and Medicine, 2018; Transportation Research Board and National Academies of Sciences, Engineering, and Medicine, 2021). Plug-in chargers, as the name suggests, must be manually connected to a vehicle. These are the least expensive variety of charger, and power output ranges from 40 to 120 kW (Transportation Research Board and National Academies of Sciences, Engineering, and Medicine, 2018). Overhead conductive chargers connect the bus to an overhead power source using a pantograph, a mechanical arm that connects the bus and charger automatically. These systems offer the maximum charging power currently available (Transportation Research Board and National Academies of Sciences, Engineering, and Medicine, 2018), reaching up to 600 kW (New Flyer Infrastructure Solutions, 2021). Wireless charging systems are typically embedded into the roadway and are used for on-route charging. Despite their lower power output in comparison to conductive chargers, wireless systems have some advantages because they do not require a physical connection between bus and charger. This decreases the time and effort required to charge and makes frequent on-route

charging (for example, at all bus stops) a possibility (Transportation Research Board and National Academies of Sciences, Engineering, and Medicine, 2021). All three charging approaches can be utilized in either depot/overnight or on-route/high-speed charging; however, plug-in charging is most commonly used for low-power depot chargers, whereas overhead and wireless charging are typically used for on-route charging (Transportation Research Board and National Academies of Sciences, Engineering, and Medicine, 2021).

Among both the research and practice communities, there is a well-documented concern about the financial viability of BEBs in comparison to conventional bus technologies. Because BEBs have only recently seen adoption in the U.S. and have an expected lifespan of 12 years (Johnson, et al., 2020; Quarles, et al., 2020; Transportation Research Board and National Academies of Sciences, Engineering, and Medicine, 2018; Transportation Research Board and National Academies of Sciences, Engineering, and Medicine, 2021), empirical assessments of life-cycle costs are not yet available. Several studies have attempted to estimate the cost difference between BEBs and other bus technologies to fill this knowledge gap. Rupp et al. (2020) performed a life-cycle emissions and cost comparison between electric and diesel buses in Aachen, Germany, and found that despite greatly reducing emissions, BEBs were not cost-competitive, even when their charging was optimized to lower electricity costs. Quarles et al. (2020) performed a similar comparison for the Capital Metropolitan Transportation Authority in Austin, Texas, and found that BEBs were not yet cost-competitive with diesel buses, but they were predicted to be competitive by 2030. Tong et al. (2017) assessed the lifetime costs and emissions of various alternative-fuel buses, including BEBs, relative to those of diesel and hybrid buses. They found that BEBs had lower operating costs but higher overall costs than conventional buses, but with the 80 percent funding assistance that many agencies receive, lifetime BEB costs were around 20 percent lower than those of diesel buses.

Blynn (2018) studied 12 transit agencies across three U.S. states and found that life-cycle costs were lower for BEBs than for hybrid buses in all cases, and lower than those of diesel buses in most cases. The National Renewable Energy Laboratory (NREL) developed a BEB financial analysis tool called VICE-BEB and applied it to a baseline scenario meant to be representative of a small fleet of BEBs for a typical American transit agency (Johnson, et al., 2020). For this baseline scenario, the life-cycle cost of a BEB fleet was found to be less than that of an equivalent diesel fleet, with the higher capital costs of BEBs and charging infrastructure

being recovered by reduced operational costs in 3.6 years. However, 5esp study assumed that a $375,000 grant per vehicle was awarded based on typical awards from the FTA Low-No program (Federal Transit Administration, 2015), without which the diesel buses would have had lower life-cycle costs.

While these analyses did not always yield the same conclusions, research and practical experience have collectively illustrated some clear principles related to the financial viability of BEBs. First, capital costs are a major obstacle in BEB adoption and the primary disadvantage of this technology in comparison to diesel or hybrid buses. Second, BEBs are becoming more cost-competitive with time as technology evolves and prices decline (Quarles, et al., 2020; Tong, et al., 2017). Third, costs are highly dependent on certain details specific to each BEB fleet implementation, including local electricity rates and charging strategy—the type of chargers selected and the time at which buses charge (Blynn, 2018; Chen, et al., 2018; Johnson, et al., 2020; Rupp, et al., 2020). Accordingly, intelligent planning can help minimize the high capital costs associated with BEB fleet transitions. Limiting the number of buses purchased and the cost of necessary charging infrastructure can help transit agencies reclaim the costs of their investments in electrification more quickly. Given that agencies cite infrastructure costs and the added complexity of charging operations as barriers to BEB expansion (Blynn, 2018) and that decision support tools for BEB planning are limited (Transportation Research Board and National Academies of Sciences, Engineering, and Medicine, 2018), there is a clear need for models to help transit agencies develop charging infrastructure systems that limit costs while supporting good transit system performance.

1.1.2. Locating Refueling Infrastructure

While the literature focused specifically on locating electric bus charging infrastructure to date is limited, the general problem of deciding minimum-cost locations for facilities of any type has been analyzed for decades. Such problems often arise when facilities such as factories, warehouses, or distribution centers are built in order to satisfy geographically distributed customer demand, and the costs incurred to satisfy the demand depend on the distance between facilities and customers. The key trade-off to be optimized in these situations is between the cost of opening more facilities and easier access to demand (Snyder & Shen, 2019). Opening a large number of facilities incurs large upfront costs but low operational costs to serve demand, while limiting the number of facilities incurs low capital costs but high operational costs. A similar

trade-off applies to the context of charger location for BEBs: installing more chargers across a broader geographic area helps make layover charging more convenient, minimizing disruptions to service, but it also incurs greater costs.

Despite the similarity between charging infrastructure location and traditional facility location, the BEB application warrants a tailored model that fully captures the context for transit agencies. In particular, it is essential to capture the effect that layover charging has on on-time performance of buses; a good model will ensure that buses can charge with minimal interruption to their scheduled operations. Hence, buses not only need to be assigned to specific chargers that are built but also scheduled to charge at specific times to ensure that a given choice of charger location maintains good quality of service.

Outside of traditional facility location, there is a substantial body of existing literature focused on identifying optimal locations for refueling stations for Evs and other alternative fuel vehicles (AFVs) (Shen, et al., 2019). However, these efforts have tended to focus on privately owned passenger vehicles, and public transit applications have been less studied. The majority of efforts in this field have modeled demand as a function of traffic flow, treating vehicle operators and refueling stations as separate entities and choosing facility locations that intercept as much flow as possible. Many authors have built off the foundational work of Hodgson (1990), who developed the so-called flow-capturing location model that takes origin-destination (O-D) pairs as inputs, assigns traveler flows to shortest paths, and locates a given number of facilities to capture the greatest amount of flow. More recent work has expanded on this formulation to better capture the AFV refueling problem, incorporating real-world concerns such as vehicle range (Kuby & Lim, 2005) and refueling station capacity (Upchurch, et al., 2009). Other common approaches to refueling station location, such as set covering and maximum covering/shortest path problem formulations (Wang & Lin, 2009), still generally utilize presumed O-D demands and assumptions about path choices to locate facilities based on traffic flows.

Flow-based models are appropriate when refueling station operators have no control over their customers' behavior and the majority of demand comes from passenger vehicles. However, because transit vehicles travel along fixed routes on established schedules, these approaches are not well suited for public transportation applications (Kunith, et al., 2017; Rogge, et al., 2015; Xylia, et al., 2017). While the literature on BEB charging infrastructure is relatively limited, a number of recent efforts have used simulation, optimization, or a combination of the two to

assess the feasibility of replacing existing diesel buses with BEBs and to determine locations for charging stations. De Filippo et al. (2014) built a simulation model to explore the feasibility of converting bus routes at the Ohio State University to BEB service. They used a physics-based energy consumption model for each bus and a simple queueing model to examine the bus network's performance with different numbers of chargers and different charger power outputs. Assuming a known battery capacity for all buses, they found that their network could be operated by BEBs served by one 500-kW charger or two 250-kW chargers. Rogge et al. (2015) took a similar approach to study the potential electrification of a city bus network in Muenster, Germany. They assumed charging stations were located at the terminal stops of all bus routes and simulated bus operations with different combinations of charging power output and bus battery size to determine the technology requirements for all buses to continue operating on their existing schedules.

Taking a different approach, Xylia et al. (2017) used optimization methods to identify locations for on-route fast charging stations in Stockholm's bus network. They considered all bus stops as candidate sites and constrained charging duration to a maximum of 5 minutes per stop. These decisions were made alongside choices of the type of fuel used on a route; each could be served by BEBs, biodiesel, or biogas buses, with BEBs having the least cost. The approach ensured that buses had enough energy to complete required service, but did not consider other concerns such as adherence to existing timetables. Kunith et al. (2017) performed a similar study with a case study applied to Berlin. They used an optimization model to choose fast charging station locations as well as bus battery capacities. As with similar works, existing bus stops were considered as the candidate locations for charging infrastructure.

Some researchers have taken on the broader problem of scheduling bus operations for BEB systems, which may also include other decisions such as charging infrastructure location. Janovec and Kohání (2019) proposed a model to schedule BEB operations, including assigning trips to blocks and planning the sequencing of charges within a block. Charging station locations are assumed to be known in advance, and the sequence of charges at each site is tracked to ensure that there are no conflicts at chargers. The resulting model is a mixed-integer linear programming problem. Alwesabi et al. (2020) developed a model to schedule electric bus operations, as well as optimize battery capacities and locate dynamic wireless charging facilities. Iliopoulou et al. (2019) examined a bus network design problem for electric buses that designed

routes and located chargers along them. The resulting formulation is a difficult bilevel optimization problem that is solved by using multi-objective particle swarm optimization.

The model most similar to those presented in this report appears to be by An (2020). An's model assumes that vehicles may charge only between trips and that the existing schedule for diesel bus operations is maintained. Using a stochastic integer programming approach, the model determines optimal charging station locations and BEB fleet size based on random energy consumption and time-of-use electricity pricing. The model does not directly schedule charging operations for each bus under study; instead, it aggregates demand at the terminal stops of trips based on battery level and locates charging stations to meet this demand. The capacity of charging stations is accounted for by establishing discrete blocks of charging time that can be booked by buses and ensuring that the total number of available blocks for a given time interval is not exceeded.

1.1.3. Queue Modeling

Because EV chargers have limited capacities, queues may form at chargers when buses that arrive find that a charger is already occupied. Agencies making decisions about where and when to charge buses therefore benefit from good estimates of how long a bus can expect to wait in a queue each time it visits a station. Generating these estimates is related to the established subject of queueing theory, which has been studied and used in practice across many fields. Classical queueing models consist of a *server* that provides some type of service to *customers,* who form a queue according to a specified discipline, such as first-come, first-served. Typically, both the arrival and service processes are influenced by external factors that cannot be controlled directly, so both are represented using random variables. The common notation used to represent queueing systems is structured as input/service/number of servers. For example, M/G/1 refers to a system in which arrivals follow a Poisson distribution, service times have a general distribution, and there is one server (Bhat, 2015). Detailed queueing models based on stochastic processes sometimes give rise to closed-form expressions for key performance metrics, such as the average length of the queue or average time spent waiting in the queue. For example, for an M/M/1 queue in which customer arrivals are Poisson with arrival rate λ and the server process is exponential with rate μ, the expected waiting time in the queue is $W_q = \frac{\lambda}{\mu(\mu-\lambda)}$ (Bhat, 2015).

There do not appear to be any examples in the currently published literature of queue models incorporated into optimization models for locating BEB chargers. However, several

researchers have applied the results of queueing theory to inform models of electric passenger vehicle charging. Many of these examples come from the literature on the electric vehicle routing problem (EVRP) or electric taxi operations. Keskin et al. (2019) used an M/G/1 queueing model at each charger to decide which public charging stations a fleet of EVs should use to complete a set of deliveries with time windows at minimum cost. Keskin et al. (2021) proposed a similar model for electric vehicle routing with time windows that included a recourse procedure for preserving feasibility when large queue delays would make deliveries late. An M/G/1 queue model was again used to calculate expected waiting times in a first-stage decision problem, while a second-stage model used simulation to obtain exact waiting times for each charger visit and construct a new feasible solution using the recourse procedure.

Besides queue models and simulation, some research has taken different approaches to account for charger capacity in optimization models. Sweda et al. (2017) proposed an adaptive routing problem for electric vehicles in which each potential charging station has a specified probability of being either available or occupied; if the station is occupied, then the driver must wait for some amount of time that is itself a random variable. For a type of EVRP, Froger et al. (2017) ensured that charging station capacities are not exceeded by adding constraints based on the Resource Constrained Scheduling Problem. Ding et al. (2015) added constraints to the EVRP that prohibit any two vehicles from utilizing a charger at the same time. These constraints are nonlinear, but they can be linearized by introducing binary variables and additional constraints.

All of the models described above focus on EV operations when chargers have already been constructed in specific locations. There have not been as many studies that have incorporated a queue model into an optimization model to identify locations for chargers. Jung et al. (2014) considered charger queues in an optimization problem for locating charging infrastructure. Their approach uses a bilevel optimization approach, with an upper-level problem of locating electric taxi chargers modeled as a queueing network and a lower-level simulation model that is used to evaluate queue times. The model is solved iteratively until the queue estimates in the upper model agree with the simulation output from the lower model. Similarly, Yang et al. (2017) used an M/M/x/s queue model in a charging infrastructure location problem for EV taxis. They used this queue model to estimate the probability that each charger is available when a taxi intends to use it and added a constraint to their optimization model to ensure that the probability of charging at some point throughout the day is sufficiently large. The

model is solved by first approximating this probability with an exponential regression and by applying a logarithmic transformation to obtain an integer linear program. These two models were the only ones identified in the electric vehicle literature that combine the consideration of queue wait times with facility location.

1.1.4. Summary

Because the existing literature on charging facility location for BEBs is quite limited, there are some notable gaps. First, the small number of models focuses on different types of charging behavior such as on-route fast charging and lower-power layover charging when a bus is out of service. Consequently, options are even more limited for practitioners seeking a model appropriate for infrastructure planning. Exacerbating this issue, additional decisions beyond charger location—including fuel type (Xylia, et al., 2017), battery size (Kunith, et al., 2017), and fleet size (An, 2020)—are often incorporated into optimization models, which may limit their applicability. Furthermore, models do not always account for all practical concerns. These include vehicle schedules and their influence on available time for charging, the limited capacity of individual charging facilities, and uncertainty in model parameters such as vehicle energy consumption, which depends on random variables that include passenger load and outdoor temperature (An, 2020).

1.2. Contribution

On the basis of the shortcomings of the existing literature identified in the previous section, this project proposed optimization models for BEB charging facility location that capture key drivers of cost and performance while limiting complexity. The main contributions of the work are as follows:

1. Two broadly applicable models for BEB charging station location that
    - Rely only on easily obtained data
    - Reflect actual bus schedules and seek to keep buses running on time
    - Locate chargers and plan the timing, location, and duration of necessary charges for all buses
    - Account for the limited capacity of chargers and resulting queueing behavior.
2. A discrete-event simulation model that provides accurate evaluation of queue times at chargers and resulting delays for both models.

3. A case study that demonstrates the models' applicability to an existing bus network in King County, Washington, that will be served by BEBs in the near future.

CHAPTER 2. METHODOLOGY

2.1. Mixed-Integer Linear Programming Models for Charger Location

This section describes in detail two mixed-integer linear programming formulations to determine optimal layover charging locations and to allocate buses to them.

2.1.1. Terminology, Definitions, and Assumptions

A *trip* refers to a single, one-way completion of a specified route. On a given day of service, each individual vehicle (a BEB) is assigned to a *block*, which is a series of trips to be completed sequentially by the same vehicle. A block often consists of several trips serving the same route in both directions, but it may include trips on any number of different routes, which may require the bus to travel some empty *deadhead* miles in between. Most buses run on a predefined schedule, with target arrival and departure times at all stops along each trip. Some down time between trips, called *recovery time,* is built into each block to provide required rest time to drivers, as well as to allow a bus that has been delayed to catch back up to schedule if needed. The models presented in this section assume that buses operate on such a schedule.

The BEB charging infrastructure location models described in this section are designed to identify the locations where charging stations should be built, as well as make operational decisions about how charging is performed, consistent with other facility location and location-allocation problems. Unlike past works that consider all bus stops as candidate charging sites (Kunith, et al., 2017; Xylia, et al., 2017), these models instead assume that the transit operator has identified a set of candidate locations for chargers. These could be at existing bus stops or layover facilities, or in undeveloped lots, none of which are necessarily on a bus's route. To maintain a high level of service for passengers, buses charge only in between trips when no passengers are on board. Upon completion of any trip, buses may drive a known distance to visit a charging station and charge for any nonnegative amount of time before driving to the start location of the subsequent trip. Doing so may force the next trip to depart later than scheduled. The models track this delay and seek to minimize it. Secondarily, they seek to retain as much scheduled recovery time as possible.

Following this premise, the modeling approach is based on several simplifying assumptions. These assumptions are documented in table 2.1.

Table 2.1 Assumptions made in the optimization models

Number	Assumption
1	Buses may start a trip later than scheduled due to previous charging but can never depart early.
2	Bus trip durations are known deterministically and are the same regardless of departure delay.
3	Each vehicle may visit only a single charging station in between any pair of trips in its block.
4	Battery charge is gained as a linear function of time.
5	Charging power may vary across stations but is the same for all vehicles at a given station. That is, power is not limited by the vehicles themselves but by the chargers.
6	No electric grid constraints are imposed. As much power as is needed at any given location can be delivered to vehicles charging there.
7	Buses enter service each day on time and with fully charged batteries.
8	Driving distances and times are known deterministically.
9	Exactly one charger is located at each candidate site.
10	When buses queue to charge, first-in, first-out queue discipline is applied.

We consider a set of vehicles (i.e., BEBs), V, where each vehicle, $v \in V$, is assigned to a known block that consists of K_v trips, which we represent as a set $T_v = \{1, \dots, K_v\}$. We are also given a set of candidate charging sites, S, of which we will select a subset to use for charging infrastructure.

The binary decision variable X_s indicates whether a charging station is ($X_s = 1$) or is not ($X_s = 1$) chosen to be located at site $s \in$ S. The binary decision variable Y_{vt}^s indicates whether vehicle v does ($Y_{vt}^s = 1$) or does not ($Y_{vt}^s = 1$) charge at site s after completing trip $t \in T_v$; likewise, the continuous decision variable y_{vt}^s represents the duration of this charge.

We define u_{vt} as the battery charge level of vehicle v at the start of trip t. Lastly, d_{vt} is the departure delay of vehicle v at the start of trip t (relative to that trip's scheduled start time), and d_{vt} is the recovery time that vehicle v spends idle before trip t (after completing trip $t - 1$), which is the time during which the vehicle is not driving, charging, or queueing to charge

between trips. Table 2.2 summarizes these definitions as well as variables and parameters that will be introduced later in this section.

The sections that follow provide detailed descriptions of the constraints and objective functions formulated for this problem.

Table 2.2 Notation definitions for charging infrastructure location models

Sets	
V	Buses
S	Candidate charging sites
T_v	Trips to be completed by each bus $v \in V$
T	All trips completed by all buses, $T = \cup_{v \in V} T_v$
C_{vt}^s	Precedence set of chargers occurring before bus v arrives at s after trip t
Decision Variables	
X^s	Binary indicator of whether charger installed at site s
Y_{vt}^s	Binary indicator of whether bus v charges at site s after completing trip t
y_{vt}^s	Time bus v spends charging at site s after completing trip t
q_{vt}^s	Time bus v spends queueing at site s after completing trip t
d_{vt}	Delay of bus v at start of trip t
r_{vt}	Recovery time of bus v at start of trip t
u_{vt}	Battery charge of bus v after completing trip t
Parameters	
f^s	Fixed cost to locate charger at site s
α	Cost associated with one minute of delay time
β	Relative value of recovery time (vs. delay)
$u_{v,1}$	Initial charge of bus v
$\overline{u_v}$	Battery capacity of bus v
$\underline{u_v}$	Minimum permissible battery charge of bus v
ξ_{vt}	Energy consumption rate of bus v during trip t
Δ_{vt}	Distance of trip t completed by bus v
ρ^s	Power output of charging station s
δ_{vt}^{1s}	Travel distance from charging station s to start location of trip t made by bus v
δ_{vt}^{2s}	Travel distance from end location of trip t made by bus v to charging station s
δ_{vt}^{3}	Travel distance from end location of trip t made by bus v to start of next trip
σ_{vt}	Scheduled start time of trip t made by bus v
ϵ_{vt}	Scheduled end time of trip t made by bus v

τ_{vt}^{1s}	Travel time from charging station s to start location of trip t made by bus v
τ_{vt}^{2s}	Travel time from end location of trip t made by bus v to charging station s
τ_{vt}^{3}	Travel time from end location of trip t made by bus v to start of next trip
λ	Scale parameter in linear queue model
M	"Big M", arbitrary large number

2.1.2. Charger Management

$$Y_{vt}^{s} \leq X^{s} \quad (2.1)$$

$$y_{vt}^{s} \leq M Y_{vt}^{s} \quad (2.2)$$

$$\sum_{s \in S} Y_{vt}^{s} \leq 1 \quad (2.3)$$

The optimization model must include constraints that ensure its recommended charging behavior is implementable in practice. Specifically, constraints (2.1) enforce that charging can take place only at a given site (i.e., $Y_{vt}^{s} = 1$) if a charger is built at that site ($X^{s} = 1$). Constraints (2.2) define the relationship between the charging indicator variables, Y_{vt}^{s}, and the charge time variables, y_{vt}^{s}; charging time is upper bounded by M if charging takes place and zero otherwise. Lastly, constraints (2.3) limit buses to visiting a maximum of one charging station in between trips, reflecting Assumption 3 of table 2.1.

2.1.3. Battery Charge Dynamics

To ensure that the chosen charging behavior is feasible, the model tracks the battery charge of each vehicle throughout its assigned block. First, assuming each bus starts its block fully charged, set the initial charge is set with the following constraints:

$$u_{v1} = \overline{u_v} \qquad \forall v \in V \quad (2.4)$$

For all trips that follow, charge $u_{v,t+1}$at the start of trip $t+1$ is equal to the charge at the start of trip t, plus any charging performed after trip t, minus all driving done to complete trip t and (potentially) to travel to/from a charging station. The total charge gained is the product of the charging rate, ρ^{s}, and the charging time, y_{vt}^{s}. Battery energy consumption from completing trip t is the product of the trip-specific energy consumption rate, ξ_{vt}, and the trip distance, Δ_{vt}. When a vehicle does visit a charging station, the charge lost driving to and from the station must be accounted for. The model defines δ_{vt}^{1s} and δ_{vt}^{2s} as the distances between charging site s and the start location or end location, 16especttively, of trip t made by vehicle v. On the other hand, a

vehicle that does not visit a charger may lose some charge while driving to the start of its next trip, which is a known distance δ_{vt}^{3} away from the end of the current trip. By combining these possible cases using the binary variables Y_{vt}^{s} to capture the if-else logic, the resulting constraint for charge tracking is as follows:

$$u_{v,t+1} = u_{vt} - \xi_{vt}\Delta_{vt} - \xi_{vt}\delta_{vt}^{3}\left(1 - \sum_{s\in S} Y_{vt}^{s}\right) + \sum_{s\in S}\left[\rho^{s} y_{vt}^{s} - \xi_{vt}\left(\delta_{vt}^{2s} + \delta_{v,t+1}^{1s}\right)Y_{vt}^{s}\right] \quad (2.5)$$

For all buses $v \in V$ and trips $t \in 1, \ldots, K_v - 1$.

Note that equation (2.3) ensures that after a trip, a bus can only charge at one station, i.e., $Y_{vt}^{s} = 1$ holds for at most one station for a given vehicle v and trip t. Equation (2.2) also ensures that if $Y_{vt}^{s} = 0$, then $y_{vt}^{s} = 0$ must hold.

We also include constraints to ensure that the charge level always remains between the lower and upper bounds $\underline{u_v}$ and $\overline{u_v}$, which are based on the battery capacity and the transit operator's policies. Note that the maximum and minimum battery charge obtained do not necessarily occur at the start of a trip, so these limits require specific constraints and are not simply compared against u_{vt}.

First, consider the lower bound on charge. When vehicles travel to a charging station, we need to ensure that they have sufficient battery to reach the station they visit. For some vehicle v and after trip t, the charge at this point is $u_{vt} - \xi_{vt}\Delta_{vt}$. If the vehicle charges at a candidate site s, then the charge of the vehicle when arriving at the site is $u_{vt} - \xi_{vt}(\Delta_{vt} + \delta_{vt}^{2s})$. Given all sites, the appropriate constraint is:

$$u_{vt} - \xi_{vt}\Delta_{vt} - \sum_{s\in S} \xi_{vt}\delta_{vt}^{2s}Y_{vt}^{s} \geq \underline{u_v} \qquad \forall v \in V, t \in T_v \quad (2.6)$$

On the other hand, we also need to ensure that vehicles never charge beyond their maximum capacity. This maximum is attained immediately after charging has been completed. If vehicle v visits charger s after completing trip t, then its charge at this time is $u_{vt} - \xi_{vt}(\Delta_{vt} + \delta_{vt}^{2s}) + \rho^{s} y_{vt}^{s}$. Accordingly, the formulation of this constraint is:

$$u_{vt} - \xi_{vt}(\Delta_{vt} + \delta_{vt}^{2s}Y_{vt}^{s}) + \rho^{s} y_{vt}^{s} \leq \overline{u_v} \qquad \forall v \in V, t \in T_v \quad (2.7)$$

Note that if $y_{vt}^{s} = Y_{vt}^{s} = 0$ for all s, then equation (2.7) reduces to $u_{vt} - \xi_{vt}\Delta_{vt} \leq \overline{u_v}$, which always holds.

2.1.4. Queueing at Charging Stations

Because a single charger can service only one bus at a time, it is important for charger location models to account for this limited capacity. Otherwise, multiple vehicles may inadvertently be scheduled to use the same charger at the same time, creating delays not captured by the model.

As discussed in Section 1.1.3, the behavior of queues in all types of engineering systems is a well-studied subject. However, classical queueing theory models are of limited use for the problem studied in this work. These models treat the time between arrivals at servers and the service time experienced at each server as random variables. In the BEB charging optimization problem, the key queueing parameters—arrival rate and service rate— are closely linked to the decision variables of where, when, and how long to charge. Treating these quantities as random variables obfuscates the direct control that we have to influence the queue times by changing the values of the decision variables. Further complicating this issue is that to determine a metric of interest such as expected queue time at each charger, assumptions about the distributions of these random variables need to be made, and the corresponding outputs from the model could easily violate these assumptions.

Furthermore, while certain types of queue model (e.g., M/M/1 or M/G/1) admit closed-form expressions for expected waiting time in the queue (Bhat, 2015), the average waiting time is of limited use in the transit context. It is much more useful to estimate exactly what queue time will be experienced each time a bus visits a charger. If the model makes charging decisions based on the knowledge that the average queue time at a given charger is 10 minutes but some bus that arrives actually needs to wait for 20 minutes, then that bus will likely run about 10 minutes behind schedule for its next trip. If the precise queue times had been known instead, then perhaps this bus would have planned to charge earlier in the day at a time when there was zero queueing time at the same charger.

To better estimate time-dependent queue waiting times at different chargers, this section proposes two different formulations to account for the limited capacity of chargers and resulting queueing behavior. The first, referred to as the linear queue (LQ) model, estimates the queue time experienced by each vehicle based on the time spent charging by buses that arrived earlier. This approach appears to be entirely novel, given the existing literature. The second is a conflict prevention model that adds constraints to explicitly prevent more than one vehicle from being

scheduled to charge at a given time. This premise is similar to the charger capacity constraints included in the models proposed by Ding et al. (2015) and Froger et al. (2017), but the specific formulation in this report is unique.

2.1.5. Linear Queue (LQ) Model

The approach taken by the linear queue model is to estimate the time spent queueing with a simple linear function: at any given time, the queueing time is assumed to be a linear function of the time elapsed since the first vehicle arrived at the charger and the total time that vehicles have spent charging so far. Let a_{vt}^s be the time at which vehicle v arrives at charger s after completing trip t (or an arbitrarily large value if this vehicle does not charge at s after t). Let a_{min} be the earliest arrival of any bus to s. Then the total time elapsed since the first charge is $a_{vt}^s - a_{min}$. The total time vehicles have spent charging up to this point can be expressed as $\sum_{(v',t')\in P_{vt}^s} y_{v't'}^s$ where P_{vt}^s is the set of vehicle-trip pairs arriving at s prior to v, t. Because the order of arrivals at s depends on the problem's decision variables, determining this set exactly is not trivial. To simplify this computation, we estimate P_{vt}^s *a priori* based on the assumption that trip delays d_{vt} are all zero in the optimal solution. In this case, we approximate P_{vt}^s as C_{vt}^s, where

$$C_{vt}^s = \left\{(v',t') : \epsilon_{v't'} + \tau_{v't'}^{2s} \le \epsilon_{vt} + \tau_{vt}^{2s}\right\} \quad (2.8)$$

Then, the time in queue q_{vt}^s can be set with the constraint

$$q_{vt}^s \ge \lambda \sum_{(v',t')\in C_{vt}^s} y_{v't'}^s - (a_{vt}^s - a_{min}) - M(1 - Y_{vt}^s) \quad (2.9)$$

where λ is a user-controlled parameter that defines the linear relationship between queue time and past charging time. Practically, it makes sense to restrict $\lambda \ge 1$ because queue time will always be nonzero if past charging time exceeds total time elapsed, although $\lambda < 1$ could be appropriate if more than one charger were installed at a given site (recall from table 2.1 that we assume this is not the case). As λ increases, estimates of queue time become more conservative. For a more detailed examination of the impact of λ on queue time estimates, see Section 4.2.2.

The complete set of constraints required to appropriately define the linear queue model and associated variables is:

$$a_{vt}^s = d_{vt} + \epsilon_{vt} + \tau_{vt}^{2s} + M(1 - Y_{vt}^s) \quad (2.10)$$

$$a^s_{min} \leq a^s_{vt} \quad (2.11)$$

$$a^s_{min} \geq a^s_{vt} - 2M(1 - A^s_{vt}) \quad (2.12)$$

$$\sum_{v,t} A^s_{vt} = 1 \quad (2.13)$$

$$q^s_{vt} \geq \lambda \sum_{(v',t') \in C^s_{vt}} y^s_{v't'} - (a^s_{vt} - a_{min}) - M(1 - Y^s_{vt}) \quad (2.14)$$

$$A^s_{vt} \in \{0, 1\} \quad (2.15)$$

$$a^s_{min} \geq 0 \quad (2.16)$$

$$a^s_{vt}, q^s_{vt} \geq 0 \quad (2.17)$$

Constraints (2.10) set the arrival time at each charger, which is arbitrarily large if $Y^s_{vt} = 0$. Constraints (2.11), (2.12), and (2.13) set the earliest arrival time at each charger a^s_{min} using the auxiliary binary variable A^s_{vt}. Constraints (2.14) set the queue times according to the LQ equation. The remaining constraints enforce variable domains.

2.1.6. Conflict Prevention (CP) Model

An alternative to the linear queue model is to take a more exact approach in ensuring that no two vehicles are ever scheduled to charge at the same time. To do so, this formulation defines a large number of new binary variables and related constraints. First, we slightly alter the definition of a^s_{vt} relative to the LQ approach to be the time that vehicle v starts charging at s after trip t, which will be later than arrival at s if $q^s_{vt} > 0$. Let the binary variable $P^s_{vtv't'}$ denote the precedence of the vehicle-trip pairs (v,t) and (v',t'). That is, if (v,t) arrives at s first ($a^s_{vt} < a^s_{v't'}$), then $P^s_{vtv't'} = 1$; otherwise, $P^s_{vtv't'} = 0$. If $P^s_{vtv't'} = 1$, then the model needs to ensure that (v, t) completes charging (at time $a^s_{vt} + y^s_{vt}$) before (v',t') starts charging (at time $a^s_{v't'}$). On the other hand, if $P^s_{vtv't'} = 0$, then (v',t') needs to complete charging before (v,t) starts. This logic can be encoded with the following set of constraints:

$$a^s_{vt} = d_{vt} + q^s_{vt} + \epsilon_{vt} + \tau^{2s}_{vt} + M(1 - Y^s_{vt}) \quad (2.18)$$

$$a^s_{vt} - a^s_{v't'} \leq M(1 - P^s_{vtv't'}) \quad (2.19)$$

$$a^s_{v't'} - a^s_{vt} \leq M P^s_{vtv't'} \quad (2.20)$$

$$a^s_{vt} + y^s_{vt} - a^s_{v't'} \leq M(1 - P^s_{vtv't'}) \quad (2.21)$$

$$a^s_{v't'} + y^s_{v't'} - a^s_{vt} \leq M P^s_{vtv't'} \quad (2.22)$$

$$a^s_{vt}, q^s_{vt} \geq 0 \quad (2.23)$$

$$P^s_{vtv't'} \in \{0, 1\} \quad (2.24)$$

Constraints (2.18) define the time that each vehicle starts charging, similarly to Constraints (2.10) in the LQ formulation. Constraints (2.19) and (2.20) set the appropriate value of the precedence indicator variable $P^s_{vtv't'}$. Constraints (2.21) and (2.22) enforce the appropriate conflict prevention constraint, depending on the value of $P^s_{vtv't'}$. The remaining constraints enforce variable bounds.

2.1.7. Delay and Recovery Tracking

In a fashion similar to battery charge, both the LQ and CP models must include constraints to accurately determine the start delay of each trip served by a BEB. These delays may propagate through a series of trips if there is not sufficient down time between trips to make up the delay. Likewise, the recovery time before each trip needs to be accurately tracked as well.

We assume that each bus enters service on time, so the initial delay is set with the following constraints:

$$d_{v0} = 0 \qquad \forall\, v \in V \quad (2.25)$$

The delay of any trip t+1 served by vehicle v is the difference between its actual start time and its scheduled start time $\sigma_{v,t+1}$. The start time of trip t+1 is the sum of the end time of trip t, time spent charging and queueing, driving time, and recovery time. Because we assume that bus trips are always completed in their scheduled amount of time (see Assumption 2 of table 2.1), the actual end time of trip t is the delay d_{vt} at the start of that trip plus its scheduled end time ϵ_{vt}. The driving time depends on whether charging is performed. If the bus visits charging station s, it must drive from the end point of trip t to the charging station, which requires a known time τ^{2s}_{vt}, and then from the charging station to the start location of trip $t + 1$, which requires known time $\tau^{1s}_{v,t+1}$. If no charging site is visited, then the vehicle simply drives from the end of t to the start of t+1, which requires time τ^{3}_{vt}. Note that in practice often $\tau^{3}_{vt} = 0$ when the

subsequent trip starts in the same location. Based on this logic, the resulting constraints are formulated as:

$$d_{v,t+1} = d_{vt} + \epsilon_{vt} + \sum_{s \in S} \left[q_{vt}^{s} + y_{vt}^{s} + \left(\tau_{vt}^{2s} + \tau_{v,t+1}^{1s} \right) Y_{vt}^{s} \right] + \tau_{vt}^{3} \left(1 - \sum_{s \in S} Y_{vt}^{s} \right) + r_{vt} - \sigma_{v,t+t} \quad (2.26)$$

for all buses $v \in V$ and trips $t = 1, \ldots, K_v - 1$.

2.1.8. Trips to and from the Bus Depot

In practice, all buses rely not only on opportunity charging in between trips, but also overnight charging at a central base location. Each bus's service day begins by pulling out of the bus depot and traveling to the start location of its first trip, and each bus's day ends by traveling from the end location of its final trip back to the depot. Our model needs to ensure that the energy required to complete these deadhead trips is properly accounted for in charge tracking. To incorporate these extra driving requirements, two dummy trips are introduced for each vehicle's trip set T_v: an initial trip $t = 0$ from the depot to the start of service and a last trip $t = K_v + 1$ back to the depot.

Δ_{v0}, the distance of trip 0, is the driving distance required to get from the depot to the start of trip $t = 1$. The distance to the next trip, δ_{v0}^{3}, is simply set to 0. Likewise, the driving time to the next trip, δ_{v0}^{3}, is set to 0. The models allow charging after the dummy trip $t = 0$, which requires driving distances $\delta_{v0}^{2s} + \delta_{v1}^{1s}$ and times $\tau_{v0}^{2s} + \tau_{v1}^{1s}$, which are calculated as for all other trips. However, the model assumes that vehicles leave the depot at the latest possible time, so that $\epsilon_{v0} = \sigma_{v1}$, which discourages charging from taking place at this time because there is no recovery time.

At the opposite end of the service day, $\Delta_{v,K_v+1}$is the driving distance from the end of the final trip, $t = K_v$, to the depot. In similar fashion as for trip $t = 0$, the model sets $\sigma_{v,K_v+1} = \epsilon_{vK_v}$ to discourage charging at this point but still allow it if needed, with the remaining distance and time parameters set based on actual driving requirements.

2.1.9. Objective Function

The objective function consists of two distinct cost components: fixed costs incurred on the basis of facility location decisions and operational costs resulting from charging behavior. The operational costs are assumed to depend on the total delay and recovery times across all trips

in the blocks under study. The relative importance of these different cost components can be controlled by three distinct user-specified parameters, α and β. The coefficient α can be interpreted as the monetary value of a single unit of delay time per day (with monetary units equal to those of f^s). Similarly, the coefficient β encodes the value of recovery time relative to delay. That is, if $\beta = 0.5$, then adding 2 minutes of recovery time provides as much value as reducing 1 minute of delay.

The assumption is that the transit operator's day-to-day objective is primarily to minimize the total delay across all bus trips. A secondary objective is to maximize recovery time between trips. This second component warrants some explanation and is included for two main reasons. First, it may be feasible for all charging to occur with zero delay if the required time for charging operations is low relative to the scheduled time in between trips. Some solutions that incur no delay may be preferable to others, so we need a way to distinguish them. Second, by including an objective function term that incentivizes greater recovery time, we indicate a preference for solutions that (i) are more resilient to unexpected delays and (ii) include less traveling to and from charging stations, because time spent driving necessarily reduces recovery time. Both of these are consistent with real-world preferences; the parameter β allows agencies using the model to specify their own valuation of additional recovery time relative to reduced delay. The value of this parameter should be restricted to $0 \leq \beta < 1$; if $\beta \geq 1$, then the problem would be unbounded because more recovery time can always be added at the expense of increased delay. With this approach, the objective function is then:

$$\min \sum_{s \in S} f^s X^s + \alpha \sum_{v \in V} \sum_{t=1}^{K_v} (d_{vt} - \beta r_{vt}) \qquad (2.27)$$

2.1.10. Mathematical Programming Formulation: Linear Queue Model

The constraints and objective function described in the preceding sections combine to form a complete mixed-integer linear programming formulation for the BEB charger location problem:

min	Objective function (2.27)
s.t.	Charger management constraints (2.1) through (2.3)
	Charge tracking constraints (2.4) through (2.7)

Linear queue constraints (2.10) through (2.17)

Delay tracking constraints (2.25) through (2.26)

$$X^s \in \{0,1\} \qquad \forall\, s \in S \qquad (2.28)$$

$$Y_{vt}^s \in \{0,1\} \qquad \forall\, v \in V, t \in T_v, s \in S \qquad (2.29)$$

$$y_{vt}^s \geq 0 \qquad \forall\, v \in V, t \in T_v, s \in S \qquad (2.30)$$

$$d_{vt}, r_{vt}, u_{vt} \geq 0 \qquad \forall\, v \in V, t \in T_v \qquad (2.31)$$

Most of the equations above have already been introduced and explained. Equations (2.28) through (2.31) simply add domain restrictions for all decision variables. The complete LQ model includes $3|T|(|S|+1)$ continuous variables, $|S|(2|T|+1)$ binary variables, and $|S|+|T|(5+6|S|)$ constraints.

2.1.11. Mathematical Programming Formulation: Conflict Prevention Model

As with the LQ model, the constraints and objective function described in the preceding sections combine to form a complete mixed-integer linear programming formulation for the BEB charger location problem with the CP model:

min Objective function (2.27)

s.t. Charger management constraints (2.1)-(2.3)

Charge tracking constraints (2.4) through (2.7)

Conflict prevention constraints (2.18) through (2.24)

Delay tracking constraints (2.25) through (2.26)

$$X^s \in \{0,1\} \qquad \forall\, s \in S \qquad (2.32)$$

$$Y_{vt}^s \in \{0,1\} \qquad \forall\, v \in V, t \in T_v, s \in S \qquad (2.33)$$

$$y_{vt}^s \geq 0 \qquad \forall\, v \in V, t \in T_v, s \in S \qquad (2.34)$$

$$d_{vt}, r_{vt}, u_{vt} \geq 0 \qquad \forall\, v \in V, t \in T_v \qquad (2.35)$$

Most of the equations above have already been introduced and explained. Equations (2.32) through (2.35) simply add domain restrictions for all decision variables. The complete CP model consists of $3|T|(|S|+1)$ continuous variables, $|S|(|T|^2+|T|+1)$ binary variables, and $|T|(5+3|S|+4|S||T|)$ constraints.

2.2. Solution Methods

Both mixed-integer linear programming formulations were implemented in Python using the Pyomo package (Bynum, et al., 2021; Hart, et al., 2011). Pyomo allows users to build an algebraic model of a mathematical program in Python code and then automatically converts this formulation into a standardized input format used by open-source and commercial solvers. This work used the Gurobi solver. For the linear queue model, the formulation was provided as-is to be solved using Gurobi's standard approaches. For the conflict prevention model, however, an iterative procedure was developed to solve the problem more efficiently. This approach was necessary because of the much larger number of variables and constraints present in the CP formulation resulting from the all-pairs comparison between trips.

The central idea behind the solution method is to repeatedly solve a relaxed version of the model, omitting some or all of the conflict prevention constraints (2.18) through (2.24). Once a solution has been obtained, it is straightforward to check whether any charging conflicts are present in the optimal solution by comparing the start and end times of all scheduled charges at each station. If such a conflict is identified—e.g., (v',t') starts charging at s before (v,t) finishes charging there—then constraints (2.18) are (2.24) for the indices (v',t'), (v,t). and s are added to the model. This procedure repeats until the solution to the relaxed model contains no charging conflicts. The approach is effective because while the total number of possible conflicts that could occur, $|T| \times |T| \times |S|$, is extremely large, the actual number of conflicts obtained in a solution to the relaxed problem is comparatively very small. There is no theoretical guarantee that the procedure will terminate with an optimal solution that is feasible for the original problem before all of the original constraints have been added, but experience with this method has found that the required number of iterations is typically small (less than 20) and that it is possible to solve much larger instances with this method than by solving the full problem directly with all constraints included.

2.3. Discrete-Event Simulation Model

To more robustly evaluate the performance of the optimization models in day-to-day transit operations, a discrete-event simulation was also developed for this project. The primary purposes of the simulation model are as follows:

(1) to accurately quantify the queue times experienced by any vehicles given their planned charging schedules,

(2) to understand the models' robustness to uncertainty in key parameters that are stochastic in nature, and
(3) to compare performance of the solutions obtained by the mixed-integer linear programming (MILP) models to alternatives obtained by other methods (e.g., an agency's existing plan for charger locations).

A key parameter of interest for simulation is the energy consumption rate per mile, ξ_{vt}, which depends on several random variables such as passenger load and weather conditions. While the simulation may be expanded in the future to consider uncertainty in other parameters, within this project the focus was on uncertainty in the energy consumption rate.

Discrete-event simulation is a common technique appropriate for many applications. The essential idea of discrete-event simulation is to update the simulated system and advance the clock only when some event of interest occurs (Ingalls, 2011). In the context of our problem, such an event could be the arrival or departure of a bus at a charging station, the start or completion of a trip served by a particular bus. This approach contrasts with other types of simulation in which the evolution of the system is repeatedly modeled for every time-step of fixed duration. The discrete-event approach allows for efficient computation (no calculations need to be done at times in between events) while capturing all key elements of the system and the interactions between them.

The discrete-event simulation program maintains a list of scheduled events known as the *calendar* (Ingalls, 2011). In each iteration of the program, the next event scheduled on the calendar is selected, and a predefined set of steps for that type of event is performed. These steps typically involve updating summary statistics, creating new events to add to the calendar, or removing entities from the simulation. This process is described in more detail in the next section.

2.3.2. Simulation Logic

The inputs to the simulation include all of the necessary information given to the optimization models, including bus schedules, charger locations, technology parameters, and travel distances and times. The simulation also requires some of the outputs from the optimization models: the chosen charger locations and the planned charging schedule of each bus (i.e., the optimal values of y_{vt}^{s}). The simulation program seeks to follow these outputs as closely as possible: if $Y_{vt}^{s} = 1$, then bus v will attempt to charge for duration y_{vt}^{s} at charger s after

completing trip t. However, in the simulation, there are two potential complications that can arise when this plan is implemented. First, the vehicle may arrive at s and find that the charger is occupied, forcing it to queue before charging, which the MILP model may not have anticipated. Second, if the cumulative energy consumption through trip t has been greater than expected because of random variations in ξ_{vt}, then the vehicle may run out of battery before completing trip t. In that case, an "emergency" or "unscheduled" charge must be added to the charging plan after some $t' < t$.

The complete logic of the BEB charging discrete-event simulation is presented in figure 2.1. This flowchart shows the logic applied to a single vehicle v. It enters the system in time to travel to the start location of its first trip. It then repeats the same logical loop for all trips t: the bus completes the trip and its battery level is updated according to the randomly generated energy consumption of that trip. If this is the last trip to be completed by v, then the bus simply returns to the depot and is removed from the simulation. Otherwise, the program checks whether a charge is planned to be completed after this trip, t. If not, a further check is performed to confirm that trip $t + 1$ can be completed without running out of battery. If the trip can be completed, the bus proceeds to complete the next trip.

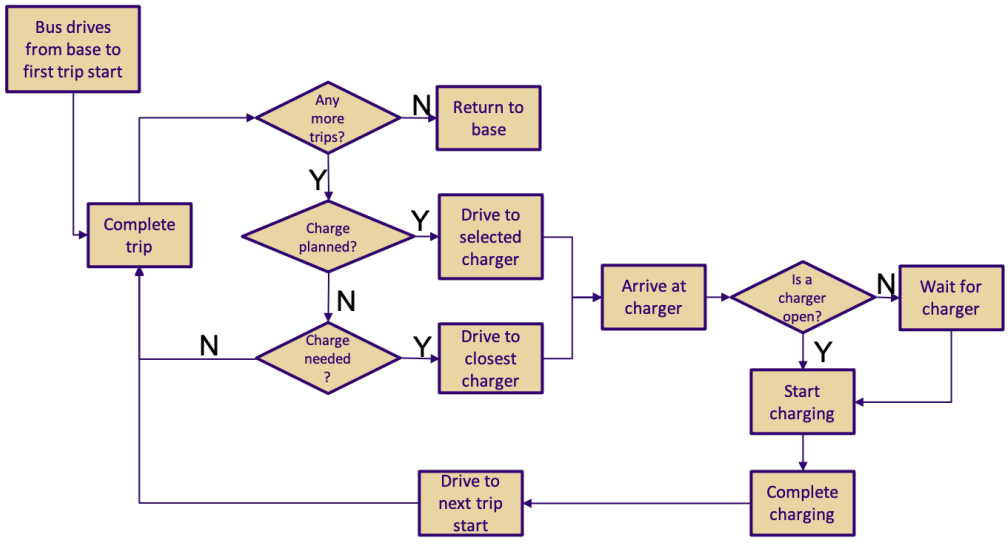

Figure 2.1 Flowchart showing logic of the discrete-event simulation

If a charge either is scheduled or is necessary because of low battery, the bus then drives to an appropriate charger—the scheduled location in the former case and the nearest charger in

the latter case. If the charger is unoccupied, the bus begins charging. Otherwise, the bus enters a queue and waits until the charger is available. Once it has completed its charge, it then drives to the start location of the next trip and follows the same logic again.

2.3.3. Emergency Charge Procedure

The simulation program identifies an emergency charge as necessary when the bus could not complete its next trip at its average energy consumption rate without its battery charge going below $\underline{u_v}$. This is a relatively simple approach; a more advanced simulation might estimate the probability that the charge level would go below $\underline{u_v}$ and set a threshold for this probability at which emergency charging would be performed.

When the simulation program detects that an emergency charge is needed, a standardized procedure is applied to decide where the bus should charge and for how long. The charging site is chosen in order to minimize the sum of deadheading time to and from the station and queueing time at the station, based on the length of the queue at the time that the decision is made. That is, when bus s needs an emergency charge after finishing trip t, the program chooses to charge at s^* such that

$$s^* = arg\min_{s} \tau_{vt}^{2s} + \tau_{v,t+1}^{1s} + q^s \quad (2.36)$$

where the queue time at s, q^s, is calculated according to the current queue. The charging time $\tilde{y}_{vt}^s$ is set in order to be sufficient to complete all remaining trips in v's block based on average energy consumption. That is,

$$\tilde{y}_{vt}^s = \left(\frac{1}{K_v}\sum_{t'=1}^{K_v} \xi_{vt'}\right) \sum_{t'=t+1}^{K_v} \left(\Delta_{vt'} + \delta_{vt'}^3\right) \quad (2.37)$$

The charging plan for vehicle v is then revised to account for this change. Since the intention is for this single emergency charge to provide enough energy for all future trips, the program sets $Y_{vt'}^s = 0$ for all $t' \geq t+1$. This emergency charging strategy is clearly suboptimal, as it does not take into account the potential delays in charging caused by the emergency charge (and opportunities to reduce delays by shifting some charge time to the future). However, it is meant to represent a reasonable recourse strategy that an agency might take when a planned charging schedule is no longer feasible.

CHAPTER 3. CASE STUDY: SOUTH KING COUNTY, WASHINGTON

Part of the transit network of southern King County, Washington, was selected as a testbed for the models presented in this report. The case study was developed in collaboration with King County Metro based on its plans for BEB expansion in this region. Metro provided some key details for the case study, including parameter values such as energy consumption per mile (based on its preliminary BEB testing) and a list of routes to be served by BEBs in the future. In total, the analysis for South King County encompassed 18 bus routes: Metro route numbers 101, 102, 111, 116, 143, 150, 157, 158, 159, 177, 178, 179, 180, 190, 192, 193, 197, and 952. Metro also identified seven candidate locations for layover chargers, which were chosen on the basis of the feasibility of installing chargers there (due to land availability, agency ownership status, etc.). Along with other publicly available information such as bus schedules and travel distances, these inputs were used to create fully defined instances of the charger location MILPs. This chapter provides additional details on the case study, data sources, and processing for application to the MILP models.

3.1. Data Collection

Several data sources were utilized in developing the case study of future BEB routes in South King County. First, Metro provided some key information, including seven candidate charging station locations throughout the area. These seven sites, their names, and locations are documented in table 3.1 and figure 3.1. Both also include the location of the South Base, which is the planned base and overnight charging location for BEBs in South King County (King County Metro Transit, 2020).

Table 3.1 Candidate charger locations for the case study

Site Name	Latitude	Longitude
South Base	47.495809	-122.286190
Burien Transit Center	47.4693256	-122.3403857
Highline Community College	47.39013	-122.294324
Kent Transit Center	47.3836401	-122.2346441
Auburn Transit Center	47.3069193	-122.2316235
South Renton Park & Ride	47.4718414	-122.2147887
Green River Community College	47.313004	-122.1805591
Federal Way Transit Center	47.3179917	-122.3056636

Figure 3.1 Map of candidate charging sites considered in the case study, plus the depot at South Base

The majority of the data needed to test the model—including bus blocks, trip schedules and distances, and stop locations—were publicly available through the Metro website via the General Transit Feed Specification (GTFS) (Google Transit APIs, 2020). Driving distances and times were calculated on the basis of free-flow conditions by using the Google Maps Distance Matrix API. This could be improved by using actual (historical) bus travel times for each path, which was not done for the current testing. On the basis of the BEB models that Metro has purchased, the case study assumed that all vehicles were 60-ft articulated buses with 466-kWh batteries that consumed energy at a rate of 3 kWh/mile for all trips served. Furthermore, we assumed that operations should keep the battery level at a 10 percent state of charge or greater at all times to promote battery longevity and provide a basic margin of error in case energy usage was higher than expected. Table 3.2 documents the values of all model parameters and their

sources, where applicable. Note that in the case study we tracked delay and recovery time in units of minutes, which informed interpretation of the constants α and β. All candidate sites were assigned the same fixed cost, and a baseline charging station power of 450 kW was chosen, as it was in the middle of the range of high-power chargers advertised by New Flyer Infrastructure Solutions (2021).

Table 3.2 Parameter values and sources, where relevant, for the South King County case study

Parameter	Value	Source
$\underline{u_v}$	46.6 kWh	(King County, 2020)
$\overline{u_v}$	466 kWh	(King County, 2020)
ξ_{vt}	3 kWh/mi	Metro (personal communication)
σ_{vt}	Varies	(King County Metro, 2020)
ϵ_{vt}	Varies	(King County Metro, 2020)
Δ_{vt}	Varies	(King County Metro, 2020)
$\delta_{vt}^{1s}, \delta_{vt}^{2s}, \delta_{vt}^{3}$	Varies	(Google Maps Platform, 2020)
$\tau_{vt}^{1s}, \tau_{vt}^{2s}, \tau_{vt}^{3}$	Varies	(Google Maps Platform, 2020)

All data related to bus operations, including blocks, trip start and end times, and the latitude/longitude coordinates of the start and end points of each trip, were obtained from Metro's GTFS feed (King County Metro, 2020). The GTFS files used for this project were originally downloaded in February 2020 and contained operating schedules for the period of February 10, 2020, to June 12, 2020. Although more up-to-date information was available, the early 2020 schedules were chosen for the case study to avoid making charging infrastructure recommendations for the future based on recent timetables that had been revised because of the COVID-19 pandemic. The GTFS format separates transit data into several files, each with a table structure (Google Transit APIs, 2020). To extract all relevant case study parameters, the GTFS data were filtered to retain only what was relevant for the case study. First, the dataset was restricted to a typical weekday of service by filtering based on the GTFS *service_id* variable. The *trips.txt* file was used to identify all remaining trips that served the 18 routes within the scope of the case study. All unique *block_id* values across these trips were considered to be the blocks (vehicles), *V,* within the scope of the study. That is, any block that included at least one trip on one of the 18 study routes on a typical weekday was included, even the trips for which it served

another route, if it did. For each of these blocks, the corresponding set of trips, T_v, could then be identified in *trips.txt* based on the *block_*id and sequenced in the order $1,\ldots,K_v$ based on the *trip_sequence* variable in *block_trip.txt*. Trip start and end times were identified on the basis of the *stop_times.txt* file, while the total distance of each trip and start/end coordinates came from *shapes.txt*.

The case study assumed that exactly one charger was being considered for installation at each candidate site. This assumption could be relaxed by creating copies of each candidate site if desired. Filtering down the GTFS data identified a total of 204 blocks serving the case study routes on a typical weekday. Of these 204 blocks, 35 would require charging at some point during the day in order to be completed, given their trip distances from GTFS and the energy parameters documented in table 3.2. Together, these 35 blocks included 401 unique trips. Hence, for the case study, $|V| = 35, |T| = 401$, and $|S| = 7$. On the basis of the sizes of these sets, we could easily compute the sizes of each of the MILP models in the case study.

The linear queue model consists of $3(|S||T| + |T|) = 9{,}624$ continuous variables, $|S|(2|T|+1) = 5{,}621$ binary variables, and $|S|+5|T|+6|S||T| = 18{,}854$ constraints. The conflict prevention model consists of $3(|S||T| + |T|) = 9{,}624$ continuous variables, $5(|T|^2 + |T| + 1) = 1{,}128{,}421$ binary variables, and $5|T| + 3|S||T| + 4|S||T|^2 = 4{,}512{,}854$ constraints. Recall that conflict prevention constraints are added to the model only as needed when conflicts are detected, so only a small fraction of these millions of possible constraints are included in the final model that is solved.

To provide some additional context for the case study, Figure 3.2 and figure 3.3 provide some visualizations of the trips in the case study over a map of the region. Figure 3.2 displays a heatmap of all trips in the case study. The blue lines trace the trips completed by all blocks in the case study based on the GTFS data. The opacity of each line corresponds to the number of trips traversing that path. The majority of routes under study traveled between South King County and Downtown Seattle. Figure 3.3 plots the start and end locations of each trip, marked with blue circles. These locations were generally more significant to the model than the full trip shapes from figure 3.2 because buses would charge only in between trips, so these locations indicate where buses tend to be located when they are available to visit a charger. The size of the marker for each trip end indicates how many individual trips ended at the same location. It is clear from figure 3.3 that the Burien Transit Center, Kent Transit Center, and South Renton Park & Ride

were especially convenient to a large number of trips, so it was expected that the model would tend to place charging infrastructure at some or all of these sites, depending on cost.

Figure 3.2 Heatmap of trips completed by BEBs in the case study

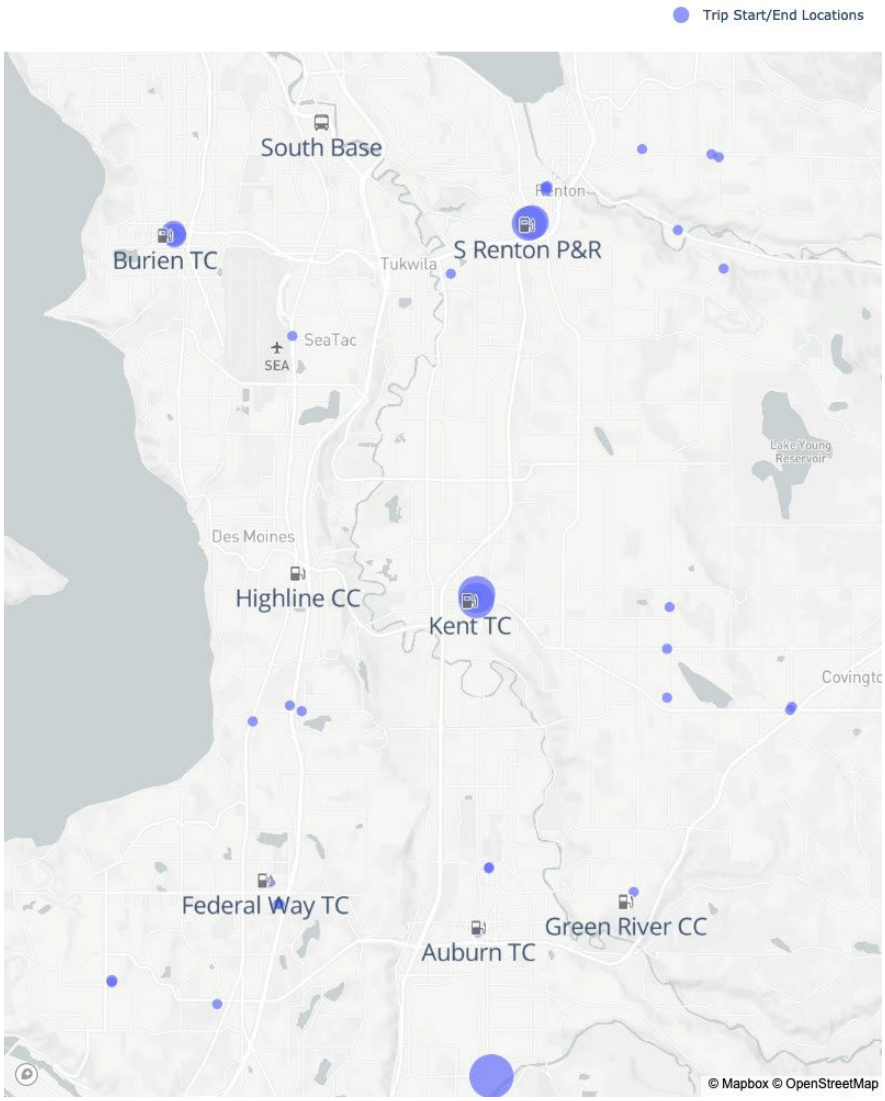

Figure 3.3 Locations of trip endpoints and candidate charging sites for the South King County case study

CHAPTER 4. RESULTS

This chapter presents the results of the case study obtained by using both the linear queue and conflict prevention MILP models, as well as a more detailed assessment of their performance obtained through discrete-event simulation.

4.1. Summary Findings

Key results from both MILP models for the South King County case study are summarized in table 4.1. Solution times were obtained on a desktop PC with a 3.4-GHz Intel Core i7 processor with 16 GB of RAM. In both cases, the Gurobi solver was able to find an optimal solution in an acceptable amount of time; however, the LQ solution took roughly five times longer. It is therefore clear that despite the greater number of binary variables and constraints in this model, the solution method described in Section 2.2 is effective in handling the complexity. Both models selected the same set of three charging infrastructure locations as optimal, but they recommended slightly different charging strategies within the day. The conflict prevention model recommended a slightly larger number of charges of shorter duration in order to limit queue delays. The delay and recovery time values reported in table 4.1 were obtained by exactly evaluating the solutions with the discrete-event simulation framework, although no random variation in model parameters was considered. This is an important distinction to make because while both models attempt to track delay and recovery times internally, the values of these quantities in the LQ model may be inaccurate if the linear queue approximation is not an accurate reflection of real queueing behavior. The conflict prevention model, on the other hand, always produces accurate assessments of delay and recovery time. In the case study scenario, both models' choices of charger locations allowed for operations without any delays due to charging. The conflict prevention model retained a slightly greater amount of total scheduled recovery time.

Table 4.1 Results of case study with 450-kW chargers

Metric	LQ Model	CP Model
Solution Time (s)	556	115
Charger Locations	Burien, Kent, S. Renton	Burien, Kent, S. Renton
Number of Charger Visits	51	54
Mean Charge Duration (min.)	16	15
Total Delay (min.)	0	0
Total Recovery Time (hrs.)	147.6	148.4

With both models, the facilities selected as optimal were consistent with reasonable expectations based on the trip end points shown in figure 3.3. The three facilities identified as optimal were located quite close to a large number of stops where trips begin and end, meaning that vehicles would not have to make particularly large detours to charge. We also saw that vehicles tended to make multiple short charges, with a typical duration of under 20 minutes, rather than a single long charge that would cause the ensuing trip to depart late.

To better understand the differences between the charging schedules output by the two models, figure 4.1 and figure 4.2 plot the number of vehicles scheduled to charge at each of the three stations chosen over the duration of the service day. In both cases, there was typically only one vehicle at a time scheduled to charge, as desired. The conflict prevention model successfully ensured that only one vehicle was ever scheduled to charge at a given time. However, as figure 4.1 demonstrates, with the linear queue model there were some times at which two vehicles were scheduled to use a charger at the same time at two of the three locations, resulting in unexpected queueing. It is a key limitation of the linear queue model that there is no guarantee that multiple vehicles will not be scheduled to charge at the same time. However, for the baseline case, there was evidently sufficient recovery time available for the vehicles that face additional queue time so that no departure delays were incurred, since the total delay was still zero.

Further analysis with the discrete-event simulation model also helped assess the robustness of each model to uncertainty. The analysis was rudimentary but provided some valuable information on how the models might handle real-world variation in model parameters. After a solution was obtained with each of the MILP models, the choice of charger locations and planned recharging strategy was used as an input to the simulation model. The simulation was then run 100 times, in which every trip in the study was assigned an energy consumption rate that was sampled from a normal distribution $N(3,0.01)$ (in kWh/mile), representing a small deviation from the baseline value. The key results of this process are summarized in table 4.2.

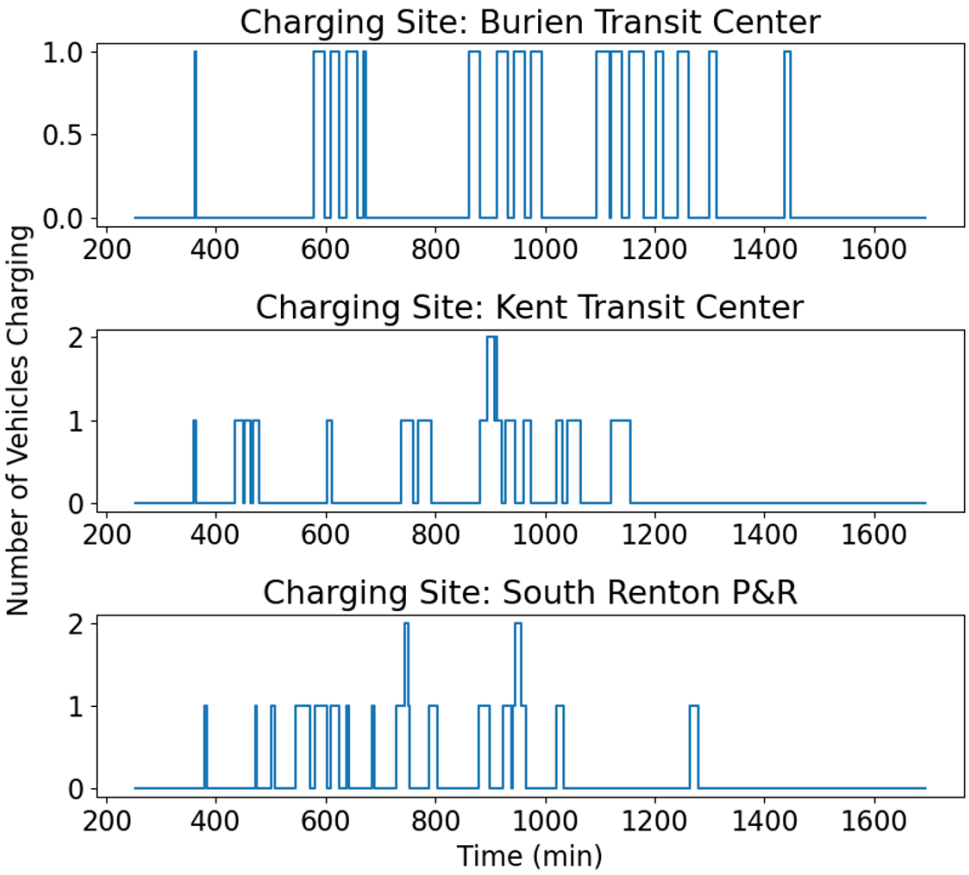

Figure 4.1 Scheduled layover charger utilization for the linear queue model solution to the case study

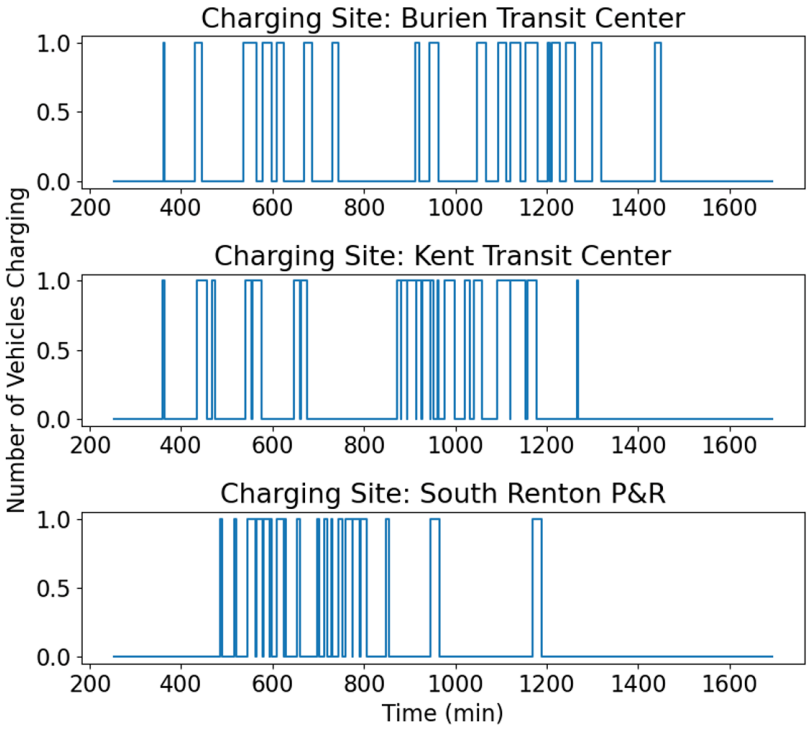

Figure 4.2 Scheduled layover charger utilization for the conflict prevention solution to the case study

Table 4.2 Performance comparison of the MILP models under uncertainty in the energy consumption rate

Metric	LQ Model	CP Model
Mean Total Delay (min.)	183	161
95% Confidence Interval	[166, 201]	[148, 174]

The results from this small simulation highlight that the model results were, in both cases, highly sensitive to actual bus energy consumption. Variations in the energy consumption rate that were quite small in comparison to the real-world fluctuations due to passenger load and environmental conditions (Transportation Research Board and National Academies of Sciences, Engineering, and Medicine, 2018) resulted in large delays for both models. Average delay was slightly lower for the CP model, but the confidence intervals indicated that this difference was not significant at the 95 percent confidence level. Regardless, it is clear that an opportunity for future work is to improve the robustness of layover charging optimization models, as both the CP

and LQ models performed much more poorly under minimal uncertainty than when all parameters were deterministic. Potential approaches for making this improvement are discussed in Chapter 5.

4.2. Sensitivity Analysis

4.2.1. Charger Power Output

As discussed in Section 1.1.1, a variety of BEB charger types with different power outputs are available commercially. The 450-kW chargers assumed in the baseline case are one commercially available option, but high-power overhead charging options offered by New Flyer, the manufacturer of Metro's BEBs, range from 150 kW to 600 kW (New Flyer Infrastructure Solutions, 2021). To examine the impact that charger power has on the model's optimal charger location decisions as well as charge scheduling, this section presents results obtained when the charging station power, ρ^s , was set to 300 kW or 600 kW. Not included were150-kW chargers because neither the LQ nor the CP model was able to converge to an optimal solution with this power level, likely because the low power forced high utilization of all chargers and greatly increased the difficulty of minimizing delays.

Table 4.3 shows the results when charger power was set to 300 kW and all other parameters stayed at the case study baseline, while table 4.4 presents the results for 600-kW chargers. In the 300-kW case, the LQ solution resulted in significant trip delays because it did not always prevent charger conflicts and created long queues. The CP solution for this model managed to avoid any delays. With 600-kW chargers, the CP solution again outperformed LQ model in terms of both delay and recovery time, although the difference was not as strong, with the LQ solution resulting in only 11 minutes of delay. In scenarios, the CP model had a faster solution time and scheduled more charges of shorter duration than the LQ model. Also, both models chose the same three sites to install chargers for each power output considered.

Table 4.3 Results of the case study with 300-kW chargers

Metric	LQ Model	CP Model
Solution Time (s)	107	83
Charger Locations	Burien, Kent, S. Renton	Burien, Kent, S. Renton
Number of Charger Visits	64	74
Mean Charge Duration (min.)	19	16
Total Delay (min.)	667	0
Total Recovery Time (hrs.)	136.5	141.0

Table 4.4 Results of the case study with 600-kW chargers

Metric	LQ Model	CP Model
Solution Time (s)	225	85
Charger Locations	Burien, Kent, S. Renton	Burien, Kent, S. Renton
Number of Charger Visits	45	48
Mean Charge Duration (min.)	13	12
Total Delay (min.)	11	0
Total Recovery Time (hrs.)	151.2	151.9

Table 4.5 presents the simulated performance of the LQ and CP models under uncertainty in ξ_{vt}. As with the baseline case, 100 simulations were run with the energy consumption rate randomly sampled from $N(3,0.01)$ kWh/mi. With 300-kW chargers, the simulation results showed that the CP model significantly outperformed the LQ model in terms of delay, as it did before accounting for randomness. In the 600-kW case, the average delay for the CP model was again lower, although the confidence intervals for the two models overlapped slightly. For each model type, 600-kW chargers yielded the lowest average delay across the three power levels considered.

Table 4.5 Simulation results with 300- and 600-kW chargers

Metric	LQ Model	CP Model
300 kW Chargers		
Mean Total Delay (min.)	858	195
95% Confidence Interval	[840, 877]	[177, 213]
600 kW Chargers		
Mean Total Delay (min.)	169	146
95% Confidence Interval	[155, 184]	[135, 158]

In summary, these results showed that for all three power levels, the CP model outperformed the LQ model in terms of delay and recovery time for the deterministic case while also achieving lower average delays for the simulations in which energy consumption rate varied. It was also solved more efficiently and provided a guarantee of actual delay and recovery times in the deterministic case. So, for the South King County case study, CP appeared to be a superior model.

Regardless of the model considered, there were clear benefits to increasing the power of chargers. Reviewing the delay and recovery time results from tables 4.1, 4.3, and 4.4, it is clear that for both models, recovery time increased as power output increased. Delay tended to decrease with power output as well, although the LQ model obtained lower delay with 450-kW than 600-kW chargers. Likewise, tables 4.2 and 4.5 show that the mean delay from the simulations decreased with charger power for each of the two models. So, as we might expect, increased charger power tended to decrease delays and increase recovery times. This result was also robust in relation to the small amount of uncertainty considered in the simulations run for the case study.

4.2.2. Linear Queue Model Parameter $\boldsymbol{\lambda}$

The choice of the appropriate value for the parameter λ in the linear queue model is not obvious without some detailed analysis. A small value of λ, especially $\lambda \leq 1$, represents an optimistic expectation of queue delays at a charger; large values of λ (e.g., $\lambda = 5$) represent a conservative estimate of queue delays that may also be harmful. To better understand the meaning of λ, first consider a simple example. Suppose vehicle v arrives at charging site s after completing trip t. Its queue time will be calculated according to Equation (2.14). Suppose that in this case, $\epsilon_{vt} + \tau_{vt}^{2s} - a_{min}^{s} = 60$ minutes; that is, vehicle v reaches charger s 60 minutes after the first vehicle to charge at s arrived there. Likewise, suppose $\sum_{(v',t',)\in C_{vt}^{s}} y_{v't'}^{s} = 30$ minutes; that is, vehicles in the precedence set C_{vt}^{s} have spent a total of 30 minutes charging at s. Then, the lower bound on q_{vt}^{s} set by Equation (2.14) as a function of λ is:

$$q_{vt}^{s} \geq \lambda(30) - 60 \text{ minutes} \qquad (4.1)$$

So in this example, the queue time will be set to zero (since $q_{vt}^{s} \geq 0$) if $\lambda \leq 2$ and will be positive otherwise. Of course, the true queue time could be either zero or nonzero, depending on how those 30 minutes of charging time are distributed. If the first vehicle to arrive charges for 30 minutes and the charger is then unoccupied for an additional 30 minutes, vehicle v will not experience any queue waiting time. On the other hand, if the first vehicle charges for 10 minutes and a second vehicle starts a 20-minute charge 10 minutes before v's arrival, then v will have 10 minutes of queueing time.

It is clear from this example that the linear queue model cannot perfectly capture the queue time in all cases, and so the challenge in selecting the appropriate λ value is to identify a value of λ that balances the likelihoods of overestimating vs. underestimating the realized queue

times. To explore this in more detail, the linear queue model was run on a modified version of the case study to explore the accuracy of predictions as a function of λ. In this modified version, all original trips were included, but only one candidate charging station (Kent Transit Center) was available. Doing so forced the model to output a solution with many nonzero values of q_{vt}^{s} (in the full case study, $q_{vt}^{s} = 0$ nearly all of the time because the model could eliminate queueing and resulting delays by constructing more chargers), which could then be compared with actual queue times obtained using the discrete-event simulation.

The results of this sensitivity analysis are provided in figure 4.3 and figure 4.4. The y-axis of figure 4.3 is the total error in queue delay estimates across all charging events. That is, if q_{vt}^{s} is the estimated queue time from the LQ model and $\tilde{q}_{vt}^{s}$ is the accurate queue time from the simulation based on the LQ solution, then the value of the total queue delay error is calculated as $\sum_{v,t,s}(q_{vt}^{s} - \tilde{q}_{vt}^{s})$. If this value is zero, then the model achieves a good balance between overestimating and underestimating queue time. Figure 4.3 shows that λ = 1.5 yielded the most accurate estimates. Smaller values of λ result in underestimated delays, while larger values produced overestimated delays.

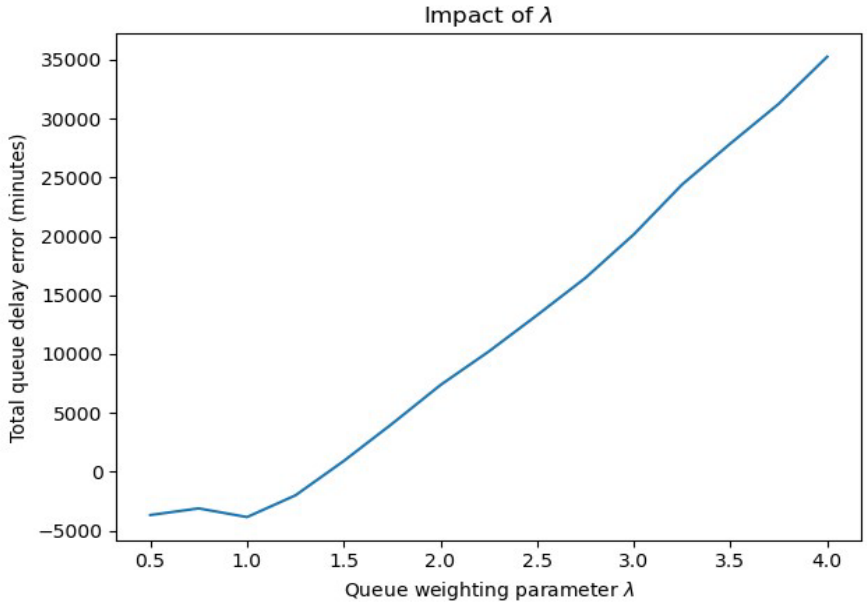

Figure 4.3 Impact of λ on the accuracy of queue time predictions

Figure 4.4 plots a different output of interest: the realized objective function value based on the delay and recovery times found with the simulation. That is, if the delay and recovery

times output by the simulation are $\tilde{d}_{vt}$ and r_{vt}, respectively, then the realized objective function value is

$$\sum_{s \in S} f^s X^s + \alpha \sum_{v \in V} \sum_{t=1}^{K_v} (\tilde{d}_{vt} - \beta r_{vt})$$

Figure 4.4 shows that for the most part, more accurate estimates of queue time corresponded to better realized objective function values. The minimum value was obtained at $\lambda = 1.25$. Lower values of λ yielded overly optimistic queue predictions that resulted in many unexpected delays due to queueing. On the other hand, large values of λ produce overly conservative estimates of queue time, which resulted in less unexpected delay but suboptimal charging plans because the model might predict an inaccurately long queue at times that would actually be convenient for a bus to charge based on the real queue time.

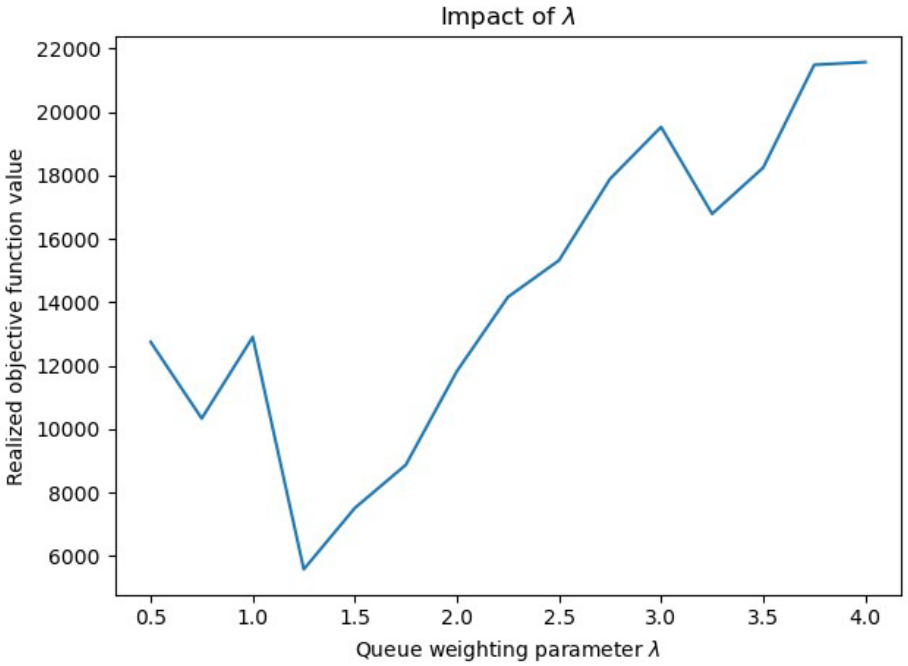

Figure 4.4 Impact of λ on the realized objective function value

CHAPTER 5. DISCUSSION AND CONCLUSION

This report presents two closely related models, referred to as linear queue (LQ) and conflict prevention (CP) models, for locating battery-electric bus charging infrastructure and simultaneously scheduling charging operations at the chosen locations. A literature review in Section 1.1 found that the existing body of research on locating charging infrastructure for buses is limited and that the small number of published works can miss some key features of charging operations for transit agencies. Accordingly, this work prioritized some improvements from the transit agency perspective. The models are based on data that can be readily obtained from agency GTFS feeds, making them easily transferable to contexts beyond the presented case study. The models also account for the limited capacity of charging stations and queueing behavior that can result, something that other authors have not addressed. Both models capture the key characteristics of an electrified transit system and can obtain solutions for the case study in a reasonable amount of time (less than 10 minutes).

The two models differ only in their treatment of queues at charging stations, so it is not too surprising that they produce similar results. The case study, regardless of the charger power output considered, showed that both models always identify the same three charger locations as optimal but differ in the planned charging schedules that they output. Running the planned charging strategies through the discrete-event simulation model found that the conflict prevention model generally has superior performance thanks to its more accurate queueing model. This difference is most notable when the utilization of chargers is very high (i.e., the 300-kW charger case), and a charging schedule conflict in the linear queue model is therefore likely to result in significant delays for multiple vehicles. Both models are not especially robust to uncertainty; running the simulation with a small variation in the energy usage rate per mile tends to result in significant delays for the solutions produced by either model.

There are likely opportunities to improve the solution times of both methods. The constraint generation approach used for the conflict prevention model had a major impact on solution times; in fact, because the case study instance contained millions of binary variables and constraints, it could not be solved as-is using Gurobi. It is likely possible to improve speed with more sophisticated approaches. Likewise, as the LQ model was solved directly with Gurobi, a tailored solution method should be able to identify optimal solutions more quickly than the current approach. Given that this model is overall smaller than the CP model, it is in some ways

surprising that its solution times tend to be longer; however, the large number of decision variables involved in the queue time constraints (2.14) is likely responsible for most of the complexity. A more sophisticated approach to solving the LQ model might intelligently relax these constraints in a manner similar to the CP constraint generation algorithm.

The results for the case study revealed that both models are not robust to small amounts of uncertainty in key parameters. Allowing the energy consumption rates to vary slightly introduced unanticipated delays, often forcing buses to charge earlier than planned because cumulative energy usage was higher than expected. The lack of robustness is not surprising because the models themselves contain no notions of uncertainty. However, in practice many of the problem parameters manifest as random variables. Energy consumption can vary widely based on passenger load, route driven, weather conditions, and more (An, 2020). Start and end times of trips are influenced by traffic conditions, passenger load, mechanical issues, and so on. An ideal model would therefore recognize that many of the parameters utilized in this project are not known exactly and would seek to provide good system performance over a wide range of real-world scenarios. There are several potential ways to extend the models to incorporate uncertainty, but two specific possibilities include simulation-based optimization similar to Jung et al. (2014) and sample average approximation (An, 2020; Kleywegt, et al., 2002).

The value of a model that incorporates uncertainty would also best be captured with a more sophisticated simulation model. A key first step for this improvement is to better understand and model the sources of uncertainty in BEB transit operations. The simulation model presented in this work treated the energy consumption rate only as a random variable and assumed it was normally distributed in the computational results. Future work could use historical data on energy consumption of buses and/or incorporate literature models of BEB energy consumption to generate more realistic energy consumption rates. Likewise, an improved simulation model would incorporate uncertainty in other parameters, such as trip start and end times. Additionally, the emergency charging procedure in the simulation as introduced in Section 2.3.2 could be made more sophisticated. Currently, the simulation results may be a bit pessimistic because the emergency charging strategy is clearly suboptimal. However, deciding where and when to charge throughout the day based on uncertain energy usage is itself a difficult stochastic optimization problem, so the right approach would need to balance improvements in these ad-hoc charging decisions with computational complexity and ease of implementation in

practice. Together, these improvements would yield a simulation model that more realistically represents day-to-day charging operations and can evaluate the performance and robustness of different solutions with a greater degree of confidence.

While there are clear future directions for improvement, the models presented in this report should still provide value to agencies looking to develop their charging infrastructure and add to the growing body of literature on decision making for BEB charging infrastructure and should operations. As transit electrification continues to take hold across the United States, such models are increasingly important and can help accelerate a transition to more environmentally friendly transit vehicles in the Pacific Northwest region, across the U.S., and around the world.

CHAPTER 6. REFERENCES

Alwesabi, Y., Wang, Y., Avalos, R. & Liu, Z., 2020. Electric bus scheduling under single depot dynamic wireless charging infrastructure planning. *Energy,* Volume 213.

An, K., 2020. Battery electric bus infrastructure planning under demand uncertainty. *Transportation Research Part C: Emerging Technologies,* Volume 111, p. 572–587.

Bhat, U. N., 2015. *An Introduction to Queueing Theory: Modeling and Analysis in Applications.* s.l.:Birkhäuser.

Blynn, K., 2018. *Accelerating Bus Electrification: Enabling a sustainable transition to low carbon transportation systems*. Master's thesis, Massachusetts Institute of Technology.

Bynum, M. L. et al., 2021. *Pyomo–optimization modeling in python.* Third ed. s.l.:Springer Science & Business Media.

Chen, Z., Yin, Y. & Song, Z., 2018. A cost-competitiveness analysis of charging infrastructure for electric bus operations. *Transportation Research Part C: Emerging Technologies,* Volume 93.

De Filippo, G., Marano, V. & Sioshansi, R., 2014. Simulation of an electric transportation system at The Ohio State University. *Applied Energy,* Volume 113, p. 1686–1691.

Ding, N., Batta, R. & Kwon, C., 2015. *Conflict-Free Electric Vehicle Routing Problem with Capacitated Charging Stations and Partial Recharge*. Technical report, University at Buffalo.

Ercan, T. & Tatari, O., 2015. A hybrid life cycle assessment of public transportation buses with alternative fuel options. *The International Journal of Life Cycle Assessment,* Volume 20, p. 1213–1231.

Federal Transit Administration, 2015. *Low or No Emission Vehicle Program - 5339(c).* s.l.:United States Department of Transportation.

Froger, A., Mendoza, J. E., Jabali, O. & Laporte, G., 2017. *A matheuristic for the electric vehicle routing problem with capacitated charging stations.* Technical report, Centre interuniversitaire de recherche sur les reseaux d'entreprise, la logistique et le transport.

Google Maps Platform, 2020. *Overview | Distance Matrix API | Google Developers.*

Google Transit APIs, 2020. *GTFS Static Overview.*

Hart, W. E., Watson, J.-P. & Woodruff, D. L., 2011. Pyomo: modeling and solving mathematical programs in Python. *Mathematical Programming Computation,* Volume 3, p. 219–260.

Hodgson, M. J., 1990. A flow-capturing location-allocation model. *Geographical Analysis,* Volume 22, p. 270–279.

Iliopoulou, C., Tassopoulos, I., Kepaptsoglou, K. & Beligiannis, G., 2019. Electric Transit Route Network Design Problem: Model and Application. *Transportation Research Record,* Volume 2673.

Ingalls, R. G., 2011. *Introduction to simulation*, p. 1374–1388.

Janovec, M. & Kohání, M., 2019. *Exact approach to the electric bus fleet scheduling.*

Johnson, C. et al., 2020. *Financial Analysis of Battery Electric Transit Buses.* Technical report, National Renewable Energy Laboratory.

Jung, J., Chow, J. Y. J., Jayakrishnan, R. & Park, J. Y., 2014. Stochastic dynamic itinerary interception refueling location problem with queue delay for electric taxi charging stations. *Transportation Research Part C: Emerging Technologies,* Volume 40, p. 123–142.

Keskin, M., Çatay, B. & Laporte, G., 2021. A simulation-based heuristic for the electric vehicle routing problem with time windows and stochastic waiting times at recharging stations. *Computers and Operations Research,* January.Volume 125.

Keskin, M., Laporte, G. & Çatay, B., 2019. Electric Vehicle Routing Problem with Time-Dependent Waiting Times at Recharging Stations. *Computers and Operations Research,* July, Volume 107, p. 77–94.

King County Metro Transit, 2020. *Battery-Electric Bus Implementation Report: Interim Base and Beyond*.

King County Metro, 2020a. *King County Metro GTFS Feed.*

King County Metro, 2020b. *Transitioning to a zero-emissions bus fleet.*

King County, 2020. *Executive Constantine announces purchase of up to 120 battery-electric buses from New Flyer of America, Inc.*

Kleywegt, A. J., Shapiro, A. & Homem-de-Mello, T., 2002. The sample average approximation method for stochastic discrete optimization. *SIAM Journal on Optimization,* Volume 12, p. 479–502.

Kuby, M. & Lim, S., 2005. The flow-refueling location problem for alternative-fuel vehicles. *Socio-Economic Planning Sciences,* Volume 39, p. 125–145.

Kunith, A., Mendelevitch, R. & Goehlich, D., 2017. Electrification of a city bus network—An optimization model for cost-effective placing of charging infrastructure and battery sizing of fast-charging electric bus systems. *International Journal of Sustainable Transportation,* Volume 11, p. 707–720.

New Flyer Infrastructure Solutions, 2021. *Charger Catalog.*

Nordelöf, A., Romare, M. & Tivander, J., 2019. Life cycle assessment of city buses powered by electricity, hydrogenated vegetable oil or diesel. *Transportation Research Part D: Transport and Environment,* Volume 75, p. 211–222.

Proterra, 2019. *Charging for Electric Fleets.*

Quarles, N., Kockelman, K. M. & Mohamed, M., 2020. Costs and benefits of electrifying and automating bus transit fleets. *Sustainability (Switzerland),* Volume 12.

Rogge, M., Wollny, S. & Sauer, D. U., 2015. Fast charging battery buses for the electrification of urban public transport—a feasibility study focusing on charging infrastructure and energy storage requirements. *Energies,* Volume 8, p. 4587–4606.

Rupp, M., Rieke, C., Handschuh, N. & Kuperjans, I., 2020. Economic and ecological optimization of electric bus charging considering variable electricity prices and CO2eq intensities. *Transportation Research Part D,* Volume 81, p. 1–15.

Shen, Z.-J. M., Feng, B., Mao, C. & Ran, L., 2019. Optimization models for electric vehicle service operations: A literature review. *Transportation Research Part B: Methodological,* Volume 128, p. 462–477.

Shi, S. et al., 2019. A life-cycle assessment of battery electric and internal combustion engine vehicles: A case in Hebei Province, China. *Journal of Cleaner Production,* Volume 228, p. 606–618.

Snyder, L. V. & Shen, Z.-J. M., 2019. *Fundamentals of supply chain theory.* Second ed. Hoboken(New): John Wiley & Sons, Inc..

Sweda, T. M., Dolinskaya, I. S. & Klabjan, D., 2017. Adaptive routing and recharging policies for electric vehicles. *Transportation Science,* Volume 51, p. 1326–1348.

Tong, F. et al., 2017. Life cycle ownership cost and environmental externality of alternative fuel options for transit buses. *Transportation Research Part D: Transport and Environment,* Volume 57.

Transportation Research Board and National Academies of Sciences, Engineering, and Medicine, 2018. *Battery Electric Buses—State of the Practice.* Washington(DC): The National Academies Press.

Transportation Research Board and National Academies of Sciences, Engineering, and Medicine, 2021. *Guidebook for Deploying Zero-Emission Transit Buses.* Washington(DC): The National Academies Press.

Upchurch, C., Kuby, M. & Lim, S., 2009. A model for location of capacitated alternative-fuel stations. *Geographical Analysis,* Volume 41, p. 85–106.

Wang, Y.-W. & Lin, C.-C., 2009. Locating road-vehicle refueling stations. *Transportation Research Part E: Logistics and Transportation Review,* Volume 45, p. 821–829.

Xylia, M. et al., 2017. Locating charging infrastructure for electric buses in Stockholm. *Transportation Research Part C: Emerging Technologies,* Volume 78, p. 183–200.

Yang, J., Dong, J. & Hu, L., 2017. A data-driven optimization-based approach for siting and sizing of electric taxi charging stations. *Transportation Research Part C: Emerging Technologies,* Volume 77, p. 462–477.

Zhou, B. et al., 2016. Real-world performance of battery electric buses and their life-cycle benefits with respect to energy consumption and carbon dioxide emissions. *Energy,* Volume 96, p. 603–613.